Open Peer Review Journal

The physics of the Earth's atmosphere II. Multimerization of atmospheric gases above the troposphere.

Michael Connolly [1]**, *Ronan Connolly*** [*1]

[1] *Connolly Scientific Research Group. Dublin, Ireland.*

Abstract

In a companion paper, a pronounced phase transition was found to occur between the troposphere and the tropopause/stratosphere regions. In this paper, it is argued that this phase change is due to the formation of multimers of the main atmospheric gases (N_2 and O_2) in the tropopause/stratosphere.

This has several implications for our current understanding of the physics of the Earth's atmosphere:

1. It offers a more satisfying explanation as to why stratospheric temperatures increase with altitude, than the conventional "ozone heating" explanation.
2. It provides an additional mechanism for the emission of infra-red and microwave radiation from the tropopause/stratosphere.
3. It suggests a faster mechanism for the formation of ozone in the ozone layer than the conventional Chapman mechanism.
4. It provides new insights into a number of weather phenomena, e.g., cyclonic/anti-cyclonic behaviour, tropical cyclones, polar vortices and the jet streams.

Citation:
M. Connolly, and R. Connolly (2014). *The physics of the Earth's atmosphere II. Multimerization of atmospheric gases above the troposphere.*, Open Peer Rev. J., 22 (*Atm. Sci.*), ver. 0.1 (non peer reviewed draft).
URL: http://oprj.net/articles/atmospheric-science/22

Version: 0.1 (non peer-reviewed)
First submitted: January 8, 2014.
This version submitted: February 14, 2014.

1 Introduction

This paper is the second in a series of three companion papers in which we revisit the conventional approaches to describing and explaining the temperature profiles of the Earth's atmosphere.

In Paper I[1] we identified a previously-overlooked phase transition associated with the transition between the *troposphere* (lower atmosphere) and the *tropopause/stratosphere* (middle atmosphere) regions. A similar phase change was also identified in the Arctic near ground level during the winter. We found we were able to obtain remarkably good fits for the atmospheric temperature profiles measured by weather balloons by just accounting for these phase transitions and for changes in humidity. Surprisingly, our fits did not require any consideration of the composition of atmospheric trace gases, such as carbon dioxide, ozone or methane. This contradicts the predictions of current atmospheric models which assume that atmospheric temperature profiles are strongly influenced by *"greenhouse gas"* concentrations. This suggests that the greenhouse effect plays a much smaller role in the atmospheric temperature profiles than has been previously assumed.

In Paper III[2], we identify a mechanism for mechanical energy transmission that is not considered by current atmospheric models, which we call *"pervection"*. We find that energy transfer within the atmosphere by this mechanism is orders of magnitude greater than conduction, convection or radiation. We propose that this rapid energy transmission mechanism is sufficient to keep the atmosphere mostly in thermodynamic equilibrium over distances of tens to hundreds of kilometres. This could explain why we were unable to detect a strong greenhouse

*Corresponding author: ronanconnolly@yahoo.ie. Website: http://globalwarmingsolved.com

effect, since the greenhouse effect theory explicitly assumes that the atmosphere is only in *local* thermodynamic equilibrium over such distances, e.g., see Ref. [3], while we found in Paper I[1] that the troposphere/tropopause/stratosphere regions are in complete thermodynamic equilibrium with each other.

In this paper, however, we will consider in more detail the identity of the troposphere/tropopause phase transition. We propose that it is due to the formation of multimers of the oxygen and/or nitrogen molecules in the atmosphere.

If oxygen and/or nitrogen multimers comprise a substantial fraction of the atmosphere in the tropopause/stratosphere, then this has a number of important implications for our understanding of atmospheric physics/chemistry as well as our understanding of the Earth's climate. A second aim of this paper will be to discuss some of these implications.

As we discussed in Paper I[1], it provides a more satisfactory explanation for the change in temperature lapse rate with altitude that occurs in the tropopause/stratosphere regions. It also provides insights into a number of important weather phenomena, e.g., cyclonic/anti-cyclonic conditions, tropical cyclones, polar vortices and the jet streams.

The formation of oxygen multimers should involve the emission of microwave radiation. This could explain Spencer & Christy, 1990's observation of unusual microwave emissions being associated with the tropopause[4]. These microwave emissions could also heat the tropopause, leading to infra-red emissions, which could be contributing to the observed spectrum for the outgoing terrestrial radiation[5].

In addition, it offers an alternative mechanism for the formation of ozone in the stratospheric "ozone layer" to the conventional Chapman cycle[6]. Similar mechanisms could also lead to the formation of some of the "NO_y" nitrogen oxides which are often associated with the ozone layer.

The format of this paper will be as follows. In Section 2 we study the conditions under which the phase transition occurs, and discuss the basis for our proposal that the phase transition involves the formation of oxygen and possibly nitrogen multimers. In Section 3, we discuss some of the implications that multimer formation has for our understanding of the physics and chemistry of the Earth's atmosphere, as well as the Earth's climate. In Section 4, we will offer some concluding remarks.

2 Characterisation and explanation for the troposphere/tropopause phase transition

2.1 Characterisation

In Paper I, by analysing several hundred weather balloon radiosondes in terms of the relationship between molar density (D) and atmospheric pressure (P), we discovered that there is a pronounced phase transition associated with the change from the troposphere to the tropopause/stratosphere regions.

For a more detailed discussion of how we identified this phase transition, and how it relates to atmospheric temperature profiles, see Paper I[1]. However, in summary, the phase transition is defined as the point at which the two linear regions of the molar density (D) versus atmospheric pressure (P) plots intersect, where the molar density is defined as the number of moles of air (n mol) per unit volume (V m^3), and has units of mol m^{-3}. The molar density at each pressure is calculated from the weather balloon data, using the ideal gas law ($PV = nRT$), as follows,

$$D = \frac{n}{V} = \frac{P}{RT} \qquad (1)$$

Where T is the measured temperature (in K) and R is the ideal gas constant (8.3145 J K^{-1}).

Figure 1 (next page) shows the phase transitions detected at a mid-latitude station (Valentia Observatory, Ireland) for seven consecutive weather balloon radiosondes over a four day period (20-23 June 2012). We can see the distinct phase transition at the pressures marked with black dashed lines, by noting that all of the observed molar densities (gray circles) to the left of the dashed lines are well fitted by one line, but to the right of the dashed lines, they are well fitted by a *different* line. As we discussed in Paper I, this phase transition coincides with a change in the behaviour of the temperature profile, i.e., to the left of the dashed lines, temperatures stop decreasing with decreasing pressure, and even start increasing with decreasing pressure.

A first step in identifying the cause of a phenomenon is to characterise the properties of the phenomenon. With this in mind, we developed a series of Python computer scripts to identify the phase transition conditions for a very large sample of radiosondes.

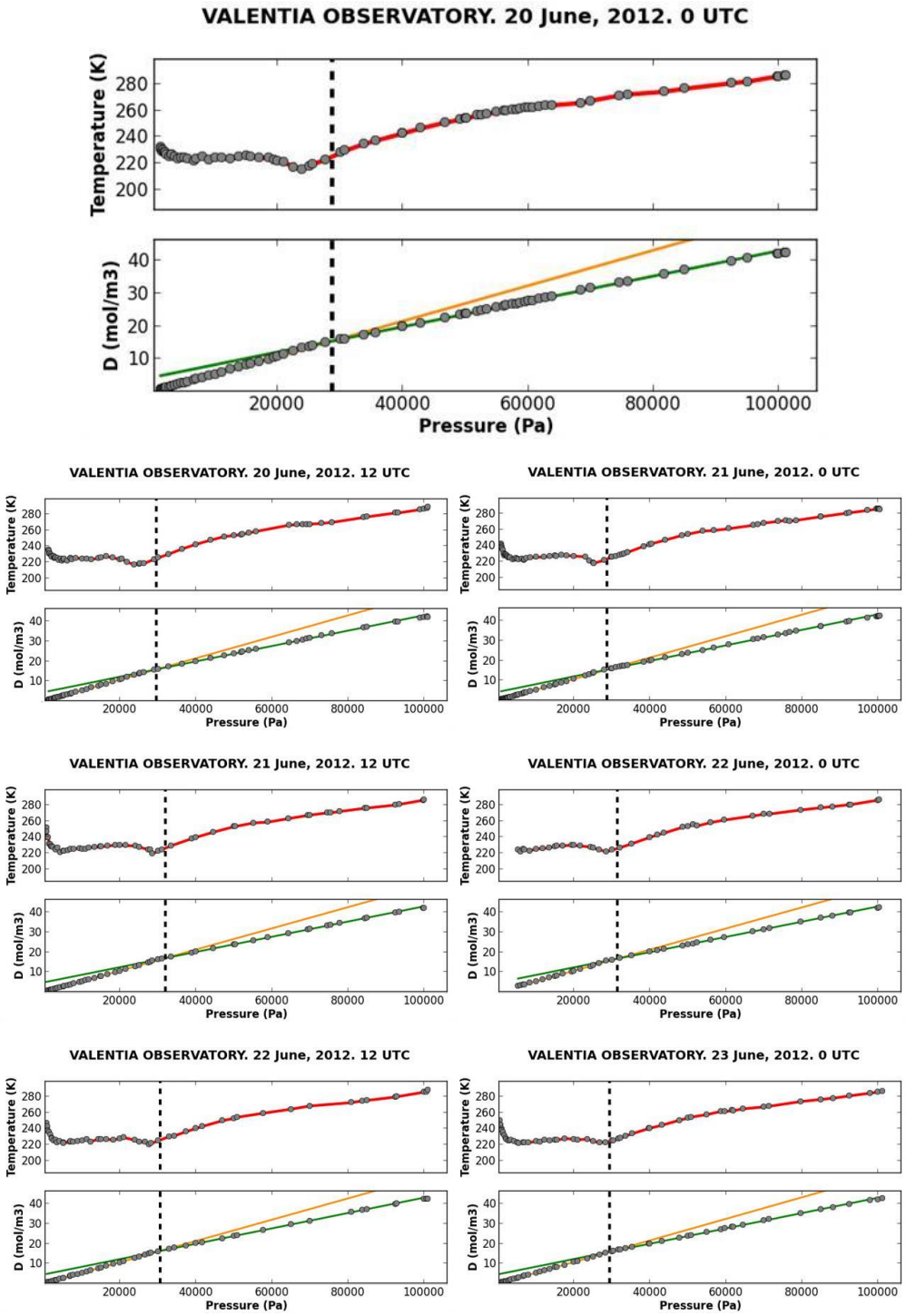

Figure 1: *Typical measurements taken from a series of twice-daily radiosonde balloons launched from Valentia Observatory, Ireland over a four-day period in June 2012. The green and yellow lines in the D versus P panels correspond to the linear slopes of the upper and lower regions. The dashed lines indicate the point of intersection of the two regions, and therefore represents the phase transition for each radiosonde. Circles correspond to the weather balloon measurements.*

We decided to use the radiosonde data from NOAA's Integrated Global Radiosonde Archive (IGRA), since:

- It was a quality controlled dataset for a large number of globally distributed stations (1,109).
- It was in a standardized format that was relatively easy to analyse with computer scripts.
- The data from each weather balloon could be separately analysed, i.e., it was not just a monthly or regionally averaged dataset (although a monthly averaged dataset was also available).

See Durre et al., 2006 for details on the IGRA dataset[7].

Since our scripts were to be run on a very large number of radiosondes ($\sim$ 13 million), it was important to allow automation. Therefore, as a simple approximation, in our scripts we estimated the slopes of the two regions (Regions 1 and 2 in Paper I[1]) by calculating the slope of the points in the region 2000-12000 Pa for Region 1 and 45000-85000 Pa for Region 2. These pressure ranges were selected on the basis of our analysis in Paper I, and through trial-and-error. Since the D/P relationship is linear for each region, only a few points are necessary to calculate the slopes of the lines. The location of the phase transition was then taken as the intersection between the two lines.

As our scripts were using an approximation to estimate the phase transition, we visually checked a large number of plots. In almost all cases in which a phase transition was calculated, the fits of the two regions appeared reasonable, and the identified transition seemed accurate.

We found in Paper I that, for polar stations, more than one phase transition can occur in the troposphere/tropopause/stratosphere regions, particularly during the winter. Initially, we considered developing scripts to identify all phase transitions for a radiosonde. However, for the purposes of this study, we decided to limit our scripts to analysing the troposphere/tropopause transition. In some cases, the scripts determined excessively high or low pressures for the "phase transition" *for polar stations*. Manual inspection of these plots revealed that this was due to the presence of multiple phase transitions. Therefore, we modified the script to remove any unrealistically high or low phase transition estimates. This appeared to counter the problem. However, we would advise the reader to use some caution in interpreting the results for the polar radiosondes, and, if in doubt, to manually inspect the plots using our scripts included in the Supplementary Information.

In some cases, there was not enough data in either the 2000-12000 Pa and/or 45000-85000 Pa regions, and so the phase transition could not be determined. This was a problem for some of the earlier radiosondes (pre-1970s), and the radiosondes from weather balloons which burst at low altitudes. In total, our scripts were able to identify the phase transition for about 70% of the radiosondes in the IGRA dataset.

We can see from Figure 1, that the pressure at which the phase transition occurs is fairly constant over the four day period ($\sim 30,000$ Pa). However, the pressure (and temperature) of the phase transition does vary somewhat from day to day. This can be seen by analysing the plots over a longer time period. As Supplementary Information, we have provided a 2 minute video showing the Valentia Observatory plots for all of 2012 at http://www.youtube.com/watch?v=UNvjqyvM0gM. We find this video is very helpful in visualising the variability in phase transition conditions, and recommend the reader views it at some stage, particularly if they are unfamiliar with the troposphere/tropopause phase transition. We include the Python scripts we used for generating these plots in the Supplementary Information. For readers familiar with the Python scripting language, it should be simple to modify the scripts to generate similar plots for other stations using the IGRA data.

Figure 2 (next page) illustrates the mean monthly variation in the pressure and temperature of the phase transition over the five year period 2008-2012, for four stations representative of:

- The Arctic - Norman Wells (NT, Canada). $65.28°N$,$126.75°W$)
- The Antarctic - Dumont d'Urville (Antarctica). $66.67°S$, $140.02°E$)
- The tropics - Changi International Airport (Singapore). $1.37°N$,$103.98°E$))
- Mid-latitudes - Valentia Observatory (Ireland). $51.93°N$,$10.25°W$).

For all stations, there are seasonal, annual cycles for both the pressure and temperature. For the Antarctic and tropical stations, the pressure and temperature annual cycles are in phase with each other, i.e., high pressures correspond to high temperatures and vice versa. For the two more northerly stations, the pressure/temperature relationship is more complex: During some parts of the year, the pressure and temperature trends seem to be in phase. However, for the rest of the year, they appear to be out of phase, e.g., the pressure maxima correspond to temperature

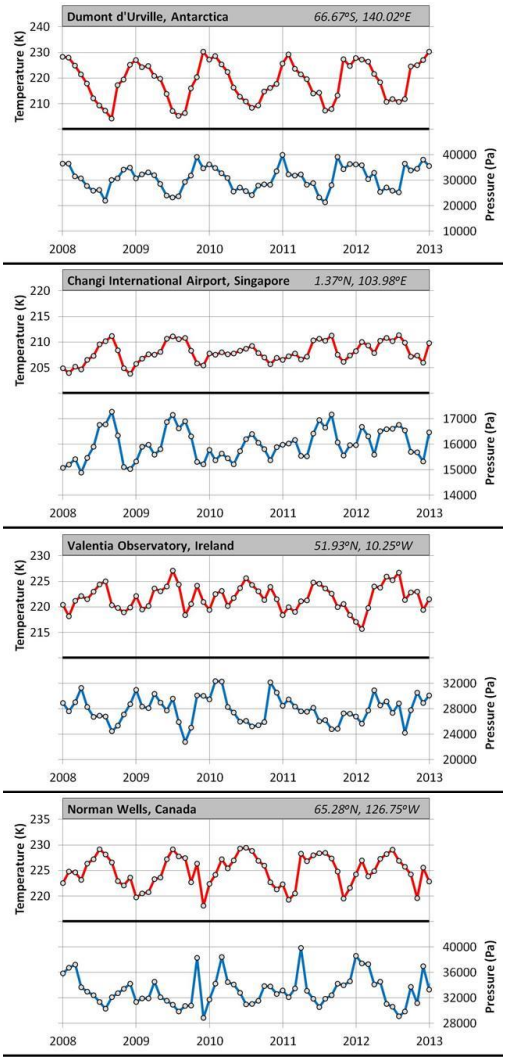

Figure 2: *The mean monthly pressures and temperatures of the phase transitions over the five year period 2008-2012 for four stations. From top to bottom: Dumont d'Urville, Antarctica; Changi, Singapore; Valentia Observatory, Ireland; and Norman Wells, Canada.*

minima, and vice versa.

We will discuss the seasonal cycles at different latitudes in more detail below. But, it is also worth noting that, for all stations, the pressure and temperature conditions vary from year to year, in terms of both the mean and range of values. In other words, just like the temperature and pressure conditions at ground level, there can be climatic variability, and even long-term trends.

Indeed, as we discussed in Paper I[1], the climate at ground level is intrinsically related to the phase transition conditions at the tropopause. Hence, researchers studying climate trends at ground level might gain insights by studying the corresponding trends in the phase transition conditions. Similarly, analysing ground temperature and pressure trends might provide insight into trends for the phase transition conditions. For interested readers, we include in the Supplementary Information the monthly mean ground temperatures, ground pressures, phase transition temperatures and phase transition pressures for all four of the stations in Figure 2, over the full station records. We also include the Python script we used for generating these monthly averages, and this can be modified to do the same for other stations in the IGRA dataset.

Although analysing the mean values for individual stations can be informative, for this paper we are interested in the mean values for the entire globe. Hence, we created a separate Python script to divide all of the 1,109 IGRA stations into 12 latitudinal zones (Figure 3), and calculate the mean phase transition conditions for each of these zones. For each station, we calculated the mean monthly conditions averaged over all available years, i.e., the *"monthly climatology"* conditions. For some stations, this involved averaging over several decades of data, while for other stations, there would only have been a few years of data.

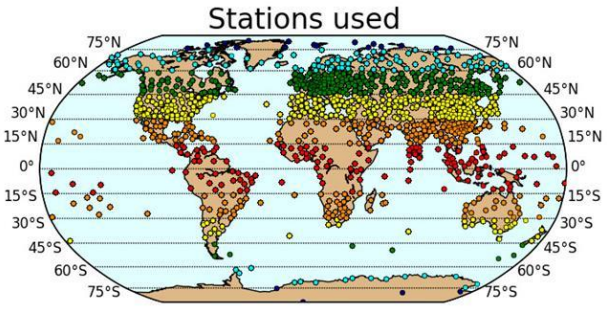

Figure 3: *Locations of the 1,109 IGRA weather balloon stations used for the analysis in this paper. Stations from different zonal latitudinal bands (15°) are colour-coded.*

Technically, the earliest available radiosonde data in the IGRA dataset is from 1946, but most stations only began collecting data in the 1960s-1970s. As a result, the mean length of the station records was only 36 years. However, since between 1 and 4 radiosondes are launched a day at most stations, this provides a large sample of radiosondes. On average,

phase transitions were identified for about 12000 radiosondes per station, and hence the climatological means discussed below are based on a total of more than 13 million radiosondes.

Zone	Temperatures (K)	Pressures (Pa)
$75-90°N$	215-231	31400-38700
$60-75°N$	218-228	30000-35100
$45-60°N$	219-226	26200-32200
$30-45°N$	219-223	20700-26300
$15-30°N$	212-217	17300-19300
$0-15°N$	207-211	15800-16800
$0-15°S$	207-209	15600-16400
$15-30°S$	212-216	17100-18900
$30-45°S$	219-223	20200-26300
$45-60°S$	220-224	26500-31300
$60-75°S$	207-229	24800-37000
$75-90°S$	198-229	18900-44900

Table 1: *The range of mean temperature and pressure conditions for the phase transition in each of the latitudinal zones.*

By their very nature, climatological means do not provide information on long term trends, since the conditions for each year are considered equivalent. However, they do provide greater statistics for studying the mean seasonal trends. Figure 4 (next page) presents the mean monthly pressure and temperature conditions for the phase transition for each of the zones. For quick reference, the maximum and minimum monthly means for each of the zones are also tabulated in Table 1.

For each of the zones, there are very distinct seasonal trends in the mean temperature and pressure of the phase transition. However, although the trends are well-defined and pronounced within each zone, there are definite differences between the trends of different zones. A detailed study of these trends and the differences between each zone is not necessary for this article. But, it may be helpful to briefly discuss some of the main features and factors that might be influencing the trends.

We should note that the ranges of the y-axes in Figure 4 are different for each of the zones. The mean temperatures and pressures of the phase transition are different for each zone, and so is the seasonal range in these values. This is more clearly seen from Table 1.

With the exception of the two Antarctic zones ($60-90°S$), there is a general tendency for the temperatures and pressures of the phase transition to increase with increasing latitude. This applies to both the minimum and the maximum values for each zone, i.e., the maximum temperatures and pressures tend to increase towards the poles, as do the minimum temperatures and pressures (see Table 1). With regards to temperature, this is the opposite to ground-level conditions, since lower latitudes tend to be warmer than higher latitudes (e.g., the tropics are warmer than the poles). It is also different from ground-level tendencies for pressure - if anything, the ground-level atmospheric pressure tends to be slightly lower at high latitudes than at mid-latitudes[8].

The seasonal range in both pressure and temperature conditions also tends to increase with latitude. For example, at $0-15°N$, the range between minimum and maximum values is only 4K and 1000 Pa, while at $75-90°N$, the range increases to 16K and 7300 Pa. For the two Antarctic zones, the mean temperature and pressure for the winter/spring months (June to November) are unusually low (Figure 4). Hence, the seasonal range is greatest for the $75-90°S$ zone at 31K and 26000 Pa.

If we now consider the seasonal trends, a number of patterns are apparent. For 7 of the 12 zones, the seasonal trends in temperature are almost exactly in phase with those in pressure. These zones include those closest to the equator: $0-15°S$ and N, $15-30°S$ and N, and to some extent $30-45°S$. Pressure and temperature also seem to be strongly correlated for the two Antarctic zones ($60-75°S$ and $75-90°S$).

Interestingly, the trends for the Antarctic zones appear to be opposite to those of the lower latitude Southern Hemisphere zones, i.e., in the Antarctic, the minimum temperatures and pressures are reached during the winter, while for the $0-45°S$ zones, this corresponds to the maximum temperatures and pressures. With this in mind, the breakdown in the correlation between the temperature and pressure trends for the $45-60°S$ zone appears to be a consequence of the transition between these two different regimes. The seasonal pressure trends for the $45-60°S$ zone seem to be quite similar to those of the $30-45°S$ zone, but the seasonal temperature trends seem to be intermediate between the zones on either side, i.e., $30-45°S$ and $60-75°S$.

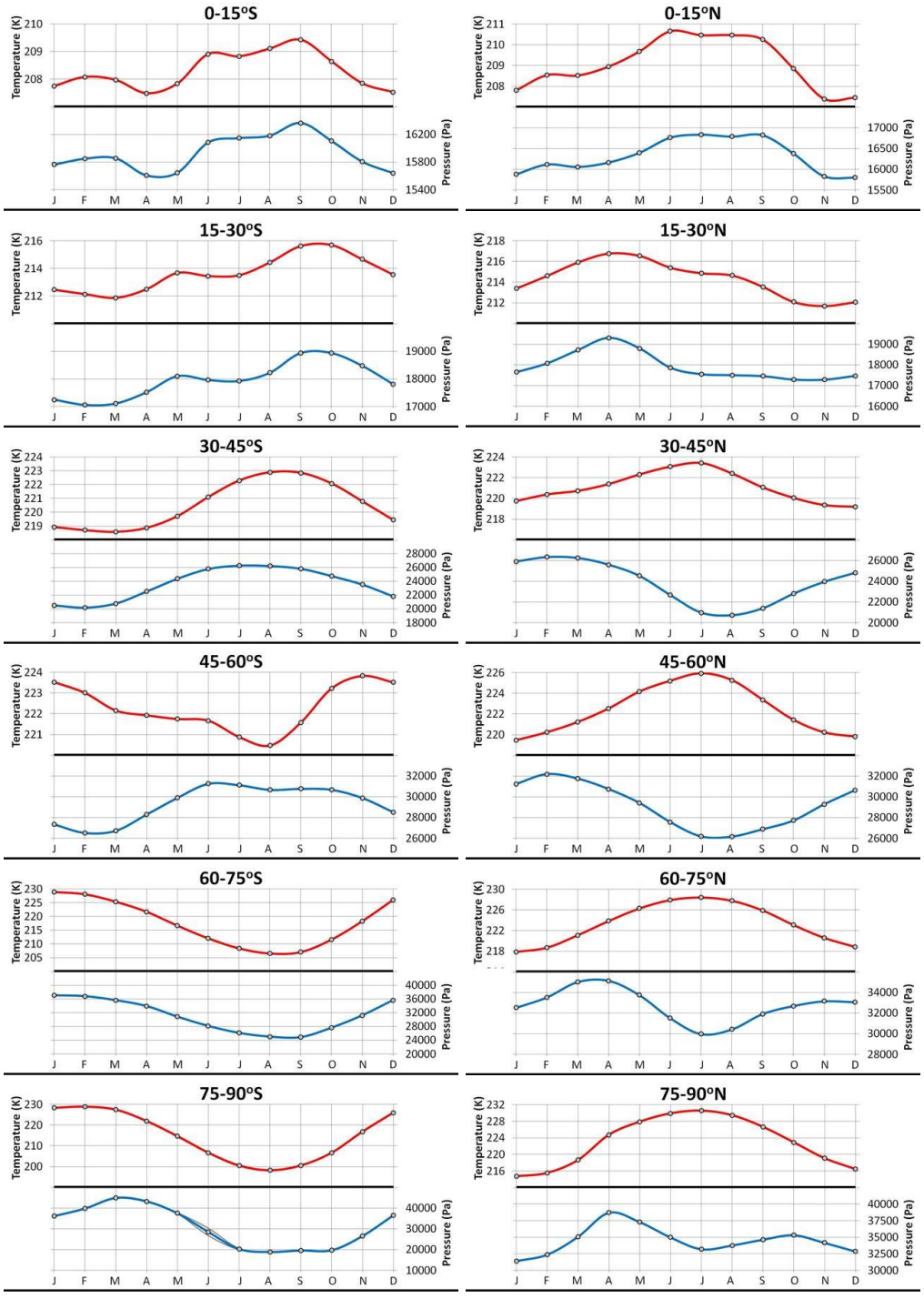

Figure 4: *Mean temperature and pressure of the phase transition by month for each of the zones in Figure 3. Confidence intervals are indicated by gray lines, but aside from some values for the low density $75 - 90°S$ zone are too small to be visible. The ranges of the y-axes are different for each zone.*

In the extra-tropical Northern Hemisphere, the relationship between the seasonal pressure and temperature trends is somewhat complex. Generally, the trends seem to be anti-correlated, with high temperatures corresponding to low pressures, and vice versa. Alternatively, it could be argued that the pressure trends "lag" the temperature trends, or vice versa. However, during the winter months, the temperature and pressure trends seem to be correlated. This winter correlation appears to increase with latitude, perhaps because the winters are most pronounced at the poles. As a result, the winter correlation seems to last from mid-October to mid-April for the $75-90^{\circ}N$ zone.

Clearly, there are a number of different factors at play in determining the mean pressure and temperature conditions for the phase transition. In Sections 2.2 and 2.3, we will briefly discuss some of the factors which could influence the phase transition conditions in light of our theory that the phase transition corresponds to the formation of oxygen and nitrogen multimers. However, before doing so, there are some factors which should be relevant, regardless of the identity of the phase transition

Generally, we would expect that lower pressures would correspond to lower temperatures, and higher pressures to higher temperatures, since temperature decreases with decreasing pressure (i.e., increasing altitude) within the troposphere - see Section 3.1.

We would also expect that changes in the local solar radiation should influence the phase transition conditions for a given region. In the Northern Hemisphere, the incoming solar radiation is at a minimum in December/January and a maximum in June/July, while in the Southern Hemisphere, the seasons are reversed. These seasonal variations strongly influence ground-level temperature conditions, particularly at higher latitudes. So, it is likely that they also play a major role in determining mean phase transition conditions, particularly at higher latitudes.

Another factor is the seasonal variation in *total* solar radiation. As can be seen from Figure 5, the total amount of solar radiation reaching the Earth currently is at a maximum in January and a minimum in July, since the Earth-Sun distance is at a minimum in January. This factor is known to change over timescales of tens to hundreds of thousands of years due to the cyclical variability in the Earth's orbit[9], and is believed to be a significant factor in the glacial to inter-glacial transitions of the ice ages[10]. At present, the difference between the January and July

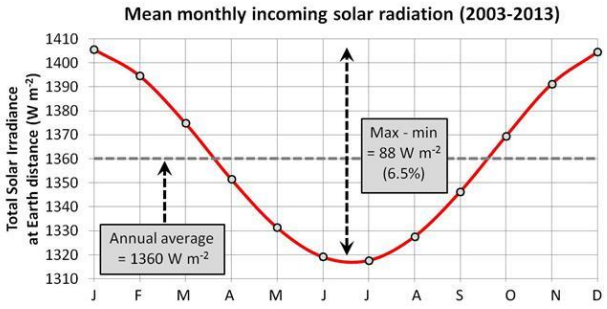

Figure 5: *Mean monthly variability of the total solar insolation at the top of the Earth's atmosphere, over the annual cycle. Values were calculated from the Total Solar Irradiance at Earth distance data from the SOlar Radiation and Climate Experiment (SORCE) satellite mission (2003-present), which was downloaded from* `http://lasp.colorado.edu/home/sorce/`.

solar radiation is quite substantial, at about 6.5% of the average solar radiation.

If the atmosphere is mostly in thermodynamic equilibrium, then we would expect that these variations in total solar insolation would influence the phase transition conditions. In Paper III, we propose that the high rates of mechanical energy transmission ("pervection") in the atmosphere allow the atmosphere to maintain thermodynamic equilibrium over distances of thousands of kilometres. This could allow any localised energy imbalances to be redistributed across the planet within a few weeks[2]. So, it seems likely that total solar insolation variations play an important role in determining the phase transition conditions.

If mechanical energy transmission allows some of the energy from the total solar insolation to become distributed throughout the atmosphere, then this would offer an additional energy source to high latitude regions during the winter months (i.e., when local solar insolation is lowest). In the Southern Hemisphere, the seasonal variation in total solar radiation coincides with the seasonal variation in local solar insolation, i.e., both are at a maximum in the austral summer and a minimum in the austal winter. Perhaps this could explain why the seasonal temperature and pressure range is greatest in Antarctica (Table 1). However, in the Northern Hemisphere, the seasonal variation in total solar radiation is opposite to the local solar insolation. Perhaps the increase in total solar radiation during the boreal winter can explain the extra-tropical Northern Hemisphere "winter cor-

relation" described above.

Of course, a major factor to consider when trying to explain the trends in the phase transition conditions, is the actual cause of the phase transition. With this in mind, let us now turn to our proposed explanation, i.e., that the phase transition involves the formation of multimers of oxygen and/or nitrogen.

2.2 Multimer formation as an explanation for the phase transition

As discussed in the previous section, the phase transition at the tropopause corresponds to an abrupt increase in the rate of decrease of the molar density of air with decreasing atmospheric pressure. Since the atmospheric pressure at any point in the atmosphere is a function of the mass of *all* of the atmosphere above that point, it seems unlikely that the rate of decrease in atmospheric pressure with altitude should change in such an abrupt manner. Instead, it seems more likely that the transition involves an increase in the rate of molar density decrease.

We can think of two mechanisms by which the rate of molar density decrease could abruptly increase:

1. The chemical composition of the air changes significantly above the tropopause.

2. The mean molecular weight of the air increases significantly above the tropopause.

Let us consider the first mechanism. Although water vapour can comprise a few percent of the atmosphere near ground level, water vapour concentrations rapidly decrease with altitude. So, water vapour is *not* a major component of the air near the upper troposphere/tropopause regions where the phase transition occurs. Dry air consists almost entirely of two gases - $\sim$ 78% nitrogen (N_2) and $\sim$ 21% oxygen (O_2), although a third gas, argon (Ar), also comprises about 1% of the air. In the troposphere/tropopause/stratosphere regions considered by our studies, the relative atomic concentrations of these three *"bulk gases"* are believed to be relatively constant with altitude[11]. Hence, the phase transition is unlikely to involve a major change in the chemical composition of the air.

On this basis, we conclude that the phase transition probably corresponds to an increase in the mean molecular weight of the air above the tropopause.

We saw in Section 2.1 that the exact conditions under which the phase transition occurs change with season, latitude, and other factors. Therefore the phase transition seems to be a reversible (and fairly rapid) process.

Also, since the atmosphere appears to obey the gas laws above as well as below the phase transition, the transition is probably a gas phase process. Although, it is possible that the phase transition could involve the formation of aerosols, i.e., very small solid particles or liquid droplets which remain suspended in the atmosphere, as occurs in clouds.

One mechanism which meets all of these requirements would be if an appreciable fraction of either the oxygen or nitrogen molecules, or both, coalesce to form higher molecular weight *"multimers"* or *"gas clusters"* through van der Waals interactions, e.g.,

$$n(A_2) \Longleftrightarrow (A_2)_n + \Delta H \qquad (2)$$

Where A is either O or N, n is the number of oxygen or nitrogen molecules (henceforth *"monomers"*) in the multimer complex, and ΔH is the heat of formation of the multimer.

Depending on the average size of n and the total fraction of the air molecules that formed multimers, this could easily increase the *average* molecular weight of the air by enough to cause a change in the rate of molar density decrease with atmospheric pressure. For small values of n, the fraction of the air that multimerises would probably need to be quite high, but for large values of n, multimers would only need to comprise a few percent (by number) of the air molecules to significantly change the average molecular weight.

The idea that atmospheric gases could form higher molecular weight van der Waals complexes under certain conditions is not new. Stable van der Waals oxygen dimers (i.e., $(O_2)_2$) have been found to exist at low temperatures, e.g., in the range $\sim 80 - 145$K[12, 13]. Molecular beam experiments have shown that the van der Waals interaction between pairs of oxygen molecules is weak, but significant[14]. The van der Waals interaction between pairs of nitrogen molecules and that between oxygen and nitrogen molecules is estimated to be similar in magnitude[15]

Indeed, oxygen dimers, nitrogen dimers ($(N_2)_2$) and mixed oxygen/nitrogen dimer complexes ($(O_2)(N_2)$) are believed to exist as stable van der Waals complexes in the troposphere/tropopause/stratosphere regions, albeit at very low trace amounts[16]. Moreover, oxygen

dimers have been measured in the atmosphere using ultraviolet-visible spectroscopy, although these dimers are believed to be only metastable complexes temporarily formed through collision processes[17, 18].

Various other high molecular weight oxygen allotropes have been calculated to have stable structures which could exist under certain conditions, e.g., see the review of Gadzhiev et al., 2013[19]. Indeed, aside from the relatively well-known three low temperature solid phases of oxygen, oxygen is also known to form at least three different solid phases under high temperature, high pressure conditions, including a tetramer form (O_8 or $(O_2)_4$) called "red oxygen" due to its observed colour - see Freiman & Jodl, 2004[20] for an extensive review of the solid phases of oxygen.

In summary, van der Waals interactions between oxygen and nitrogen molecules can become significant under certain conditions. The question is whether or not those conditions could include those at the phase transition. As we mentioned above, the van der Waals interaction between oxygen, nitrogen and mixed oxygen/nitrogen dimers has been found to be quite weak, and at the temperatures associated with the phase transition (198-231K - see Table 1), they are unlikely to be very stable. However, if the air molecules were able to coalesce to form larger multimers ($n > 2$), then the cumulative interactions of the larger van der Waals complexes might become strong enough to make the multimers stable above the tropopause. To investigate this, let us now calculate the enthalpies of formation of multimers from the monomers for different values of n, i.e., ΔH from Equation 2.

$$\Delta H = H^{products} - H^{reactants} \tag{3}$$

One way for calculating the enthalpy of formation of the multimers from the monomers would be if we could calculate the difference between the enthalpy of the monomers and the multimers. The molar enthalpy of a gas (H) is defined as,

$$H = U + PV \tag{4}$$

Where U is the internal energy of the gas, while P and V represent the pressure and volume of the gas. The internal energy of the gas is,

$$U = \frac{1}{2}\alpha RT \tag{5}$$

Where T is the temperature of the gas, $R = 8.3145$ J K^{-1} mol^{-1} is the ideal gas constant and α is the number of degrees of freedom that contribute to the internal energy of the gas at temperature T. We can see that each degree of freedom contributes $\frac{1}{2}RT$ to the internal energy of a mole of gas. In this context, a degree of freedom is an independent mode (or way) in which the gas can have energy, e.g., translation, rotation and vibration.

Since $PV = RT$ for one mole of gas (from the ideal gas law), we can combine Equations 4 and 5 to yield,

$$H = \frac{1}{2}\alpha RT + RT = \left(\frac{1}{2}\alpha + 1\right) RT \tag{6}$$

For most gases under atmospheric conditions, we only need consider translation, rotation and vibration, when calculating α, i.e.,

$$\alpha = \alpha_{translational} + \alpha_{rotational} + \alpha_{vibrational} \tag{7}$$

All gases have three translational degrees of freedom corresponding to the three spatial axes. For monatomic gases, such as argon, or the atomic forms of nitrogen and oxygen, these are the only available degrees of freedom, i.e., $\alpha = 3$ for O, N, and Ar. However, for more complex molecules, we must also consider the rotational and vibrational degrees.

The diatomic N_2 and O_2 molecules (i.e., the monomers) are linear molecules, and so only have 2 rotational degrees of freedom, while all of the multimers would have 3 rotational degrees of freedom.

Because the covalent bond in the diatomic N_2 and O_2 molecules is quite strong, the vibrational modes do not substantially contribute to the degrees of freedom *at atmospheric temperatures*. So, for the monomers, $\alpha = 5$ (3 translational and 2 rotational). Therefore, from Equation 6,

$$H^{monomer} = \left(\frac{5}{2} + 1\right) RT = \frac{7}{2}RT \tag{8}$$

Compared to the covalent bond in the monomers, the strength of the van der Waals bond in the multimers is very weak, e.g., Aquilanti et al., 1999 found the oxygen dimer bond energy to be about 17.0 meV[14]. With this in mind, let us assume that the different modes of the bond contribute fully to the degrees of freedom of the multimers at atmospheric temperatures. If we assume that the strength of the covalent bond of the monomers remains about the same in the multimer, then (as for the diatomic molecules) the modes of the covalent bond of the monomer will not contribute to the degrees of freedom. This seems a reasonable assumption, since even when oxygen

molecules are adsorbed onto fullerene surfaces, the vibrational energy of the covalent bond remains comparable to that in the gas phase[21].

If N is the number of atoms in a multimer, then the total number of vibrational modes will be $3N-6$, but $\frac{N}{2}$ of those modes will be due to the covalent bonds. So the total number of vibrational modes which contribute to the degrees of freedom of the multimer (under atmospheric conditions) will be $3N-6-\frac{N}{2}$. We must also note that each vibrational mode actually contributes *two* degrees of freedom to the internal energy of a molecule - one due to the kinetic component and one due to the potential component of the vibration. Hence, for a multimer,

$$\alpha_{vibrational} = 2(3N - 6 - \frac{N}{2}) = 5N - 12 \quad (9)$$

Since $\alpha_{translational} = 3$ and $\alpha_{rotational} = 3$,

$$\alpha = 3 + 3 + 5N - 12 = 5N - 6 \quad (10)$$

Therefore, from Equation 6, we can calculate the molar enthalpy of a multimer,

$$H^{multimer} = \left(\frac{5N-6}{2} + 1\right) RT \quad (11)$$

With this, we can now calculate the enthalpy of formation of a multimer of size n from n molecules of either N_2 or O_2, using Equation 3,

$$\Delta H = H^{multimer} - n\,(H^{monomer}) \quad (12)$$

Recalling that $n = 2N$, we can then combine Equations 8 and 11 to yield,

$$\Delta H = (5n - 2)\,RT - n\left(\frac{7}{2}RT\right) \quad (13)$$

$$= \left(\frac{3n}{2} - 2\right) RT \quad (14)$$

By substituting different values of n into Equation 14, we can construct Table 2. Alternatively, by rearranging Equation 14, we can derive a formula to estimate n from the enthalpy of formation,

$$n = \frac{2}{3}\left(\frac{\Delta H}{RT} + 2\right) \quad (15)$$

We will use this equation in Section 2.3.

The values of ΔH in Table 2 are large enough to make it plausible that, above the troposphere, a significant fraction of the air molecules could form stable multimers of some size n. In other words, our theory that the phase transition corresponds to the formation of multimers is reasonable on thermodynamic grounds. In the next section, we will consider possible values for n.

Multimer type	**Species**	α	ΔH
Atomic	$(A_2)_{\frac{1}{2}}$	3	-0.5RT
Monomer	A_2	5	0.0
Dimer	$(A_2)_2$	14	+1.0RT
Trimer	$(A_2)_3$	24	+2.5RT
Tetramer	$(A_2)_4$	34	+4.0RT
Pentamer	$(A_2)_5$	44	+5.5RT
Hexamer	$(A_2)_6$	54	+7.0RT
Septamer	$(A_2)_7$	64	+8.5RT
Octamer	$(A_2)_8$	74	+10.0RT
Nonimer	$(A_2)_9$	84	+11.5RT
Decimer	$(A_2)_{10}$	94	+13.0RT

Table 2: *Calculated heats of formation for various multimers from the two main diatomic atmospheric gases, where $A_2 = O_2$ or N_2.*

2.3 Modification of the barometric formula to estimate the size of multimers

Figure 6 presents the pressure/temperature conditions associated with the phase transition for each of the zones and months in Figure 4. In a sense, we can consider this a partial phase diagram for the atmosphere near the troposphere/tropopause boundary. Using our terminology from Paper I, we refer to the tropospheric phase of air as the "light phase". This corresponds to the region at the top of Figure 6. Below the phase transition, the air adopts what we referred to generically in Paper I as the "heavy phase"[1]. This is the phase during which we propose multimerization takes place.

In Figure 6, all of the points from a given latitude zone have the same colour and shape (triangles for the Northern Hemisphere and circles for the Southern Hemisphere). Taken collectively, the range of the conditions corresponding to the phase transition is relatively small, i.e., temperatures in the range 198-231 K and pressures in the range 15600-44900 Pa (see Table 1). When we consider a specific latitude zone, the range becomes even smaller and more defined, e.g., 207-211 K and 15800-16800 Pa for $0-15°N$. The seasonal variation for each zone is also very well-defined and periodic. This is more apparent in Figure

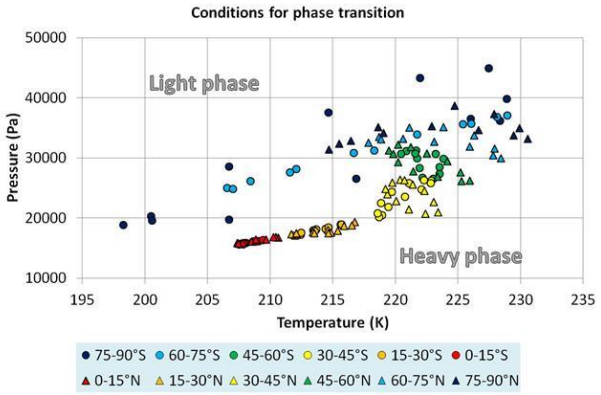

Figure 6: *Mean monthly conditions for the phase transition of each of the latitudinal zones of Figure 3. Triangles correspond to the Northern Hemisphere, and circles correspond to the Southern Hemisphere.*

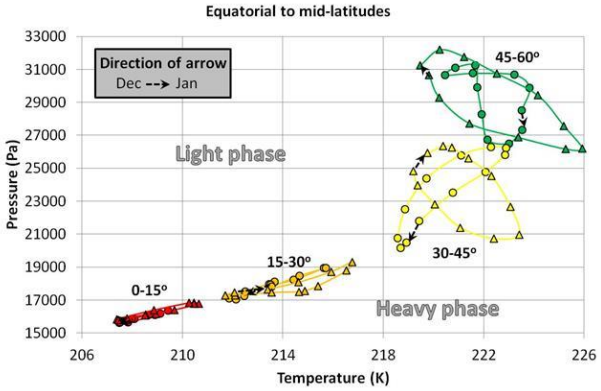

Figure 7: *Seasonal variations of the mean monthly conditions for the phase transition of the equatorial and mid-latitude zones from Figure 6. The arrows for each zone indicate the direction December to January. Triangles correspond to the Northern Hemisphere, and circles correspond to the Southern Hemisphere.*

7 where the seasonal trends in phase transition conditions are indicated for each of the low-to-mid-latitude zones.

The fact that the temperatures and pressures of the phase transition are so well-defined for each latitudinal zone suggests that there is a thermodynamic significance for the phase transition conditions in each zone. This raises the possibility that we can extract information about the nature of the phase transition (e.g., ΔH) from the pressures and temperatures of the phase transition. With this in mind, let us consider the relationship between these values and the thermodynamics of the phase transition.

The barometric formula is a well-known equation used to calculate the atmospheric pressure at a given altitude (h), or vice versa[22],

$$P = P_0 \exp\left(\frac{-mgh}{RT}\right) \tag{16}$$

Where P_0 is the atmospheric pressure at ground level (100000 Pa at standard temperature and pressure), m is the average molecular weight of air (in g mol^{-1}) and $g = 9.81$ m s^{-2} is the acceleration due to gravity.

Although the barometric formula is typically used for relating pressure to altitude, it also provides a relationship between the pressure and the ratio of gravitational potential energy (mgh) to kinetic energy (RT). Therefore, it should be useful in describing the thermodynamics of different pressure/temperature conditions. However, the formula is only valid when the only forms of energy which change in the atmosphere are kinetic energy and gravitational potential energy. It does not allow for phase changes or chemical reactions, for instance.

If we want a complete thermodynamic description of the pressure/temperature conditions, then we need to consider any other energy changes which may be involved. For instance, we saw in Section 2.2 that multimerization would alter the internal energy of the atmospheric gases. We also note that the energy of the atmosphere at a given point is also affected by many other factors, e.g., local insolation, total solar insolation, magnetic fields, and so on.

For this reason, let us generalise the barometric formula to account for changes in energy other than potential energy,

$$P = P_0 \exp\left(\frac{\Delta E}{RT}\right) \tag{17}$$

Where ΔE represents the *net* change in energy with respect to P,

$$\Delta E = -\Delta(mgh) + \Delta H + \Delta(h\nu) + \Delta(\beta\phi) + \Delta(\frac{1}{2}\rho v^2) + \ldots \tag{18}$$

Where $\Delta(h\nu)$ corresponds to a change in electromagnetic radiation, $\Delta(\beta\phi)$ corresponds to any change in magnetic field, $\Delta(\frac{1}{2}\rho v^2)$ corresponds to any change in the velocity of the air (e.g., change in wind speed), and the "..." corresponds to any other change in the internal or external energy of the air molecules. In our case, ΔH is the enthalpy of multimerization, which we calculated for different values of n in the

previous section. In the original barometric equation, $-mgh$ implicitly represented a *change* in potential energy at altitude h, relative to sea level. But, in the context of our generalised formula, it seems sensible to explicitly note that we are considering changes in energy. So, we have changed the potential energy component from $-mgh$ to $-\Delta(mgh)$. This also allows for the fact that m can change, e.g., by multimerization, as well as accounting for the fact that g slightly varies with latitude and altitude.

If the only energy component that changes is $-mgh$ then Equation 17 reverts to Equation 16. However, our generalised barometric formula allows us to also consider the influence that other energy components have on pressure. In other words, we can use it as a tool for considering the thermodynamic significance of the different pressure and temperature conditions at which the phase transition occurs.

If multimerization occurs, then this will increase ΔE by ΔH. Therefore, the pressure (and correspondingly, the temperature) at which the phase transition occurs is influenced by ΔH. So, in theory, it might be possible to estimate ΔH from Equation 17 from our phase diagram in Figure 6. However, the other energy components of Equation 18 also influence the pressure of the phase transition, at a given time and location.

Let us briefly consider some of the factors which could influence the phase transition conditions:

- The altitude at which the phase transition occurs varies with season and latitude. Therefore, the $-\Delta(mgh)$ component will similarly vary.

- We saw from Equation 14 and Table 2 that the enthalpy of multimerization depends on the size of the multimers n. Hence, if the average size of the multimers varies, then ΔH will also vary.

- As we discussed in Section 2, the local insolation varies with latitude and season, and the total solar insolation varies with season. If there are long term trends in solar activity, this could alter both terms. Hence, $\Delta(h\nu)$ can vary with latitude, season, hemisphere, and from year to year.

- The geomagnetic field varies with latitude and season. Also, there can be long term trends in the geomagnetic field. All of these factors could contribute to $\Delta(\beta\phi)$. In addition, diatomic oxygen is paramagnetic, but multimers of oxygen do not have to be. So, if multimerization of the oxygen molecules occurs, this could alter the interaction of the air molecules with the geomagnetic field, i.e., alter $\Delta(\beta\phi)$.

- In Section 3.4, we will discuss how changes in the phase transition boundary can influence wind speeds and patterns. Similarly, changes in wind speeds could influence ΔE by $\Delta(\frac{1}{2}\rho v^2)$.

There could be many more factors which significantly contribute to ΔE, e.g., changes in the atmospheric electric field[23], or changes in water vapour distribution. However, for the purposes of this article, it is sufficient to note that ΔE has many components, and as a result, there are many factors which could influence the phase transition conditions.

Nonetheless, we notice from Figures 6 and 7 that there are quite a few regions in which the pressure and temperature of the phase transitions vary linearly with each other, e.g., in the tropical and subtropical zones. This suggests that the relative contribution of each of the energy components to ΔE is fairly constant.

We can estimate the enthalpy of multimerization for these regions with linear behaviour from Equation 17. Let us take the logarithm of Equation 17,

$$\ln P = \ln P_0 + \frac{\Delta E}{RT} \tag{19}$$

If we treat $\ln P_0$ as a constant, then for regions which show linear behaviour, we can estimate ΔE as the slope from the equation of the line for a plot of $\ln P$ against $\frac{1}{RT}$. In other words, if we take the equation of the line as $y = mx + c$, with $y = \ln P$, $x = \frac{1}{RT}$ and $c = \ln P_0$, then the slope will be $m = \Delta E$.

There are several parts of our phase diagram in which there seems to be a fairly linear relationship between P and T, e.g., for the low latitude zones, and the $60 - 75°S$ zone. There is also a quite linear relationship for the $75 - 90°S$ zone, and this relationship becomes even more linear, if we divide the points into two subsets, i.e., October-February ("spring/summer") and March-September ("autumn/winter"). These are the zones in which P and T are "in phase" in Figure 4. In Figure 8, we plot Equation 19 for these different subsets of points. The slopes of these lines should give us ΔE (in units of J mol^{-1}) for these zones.

If ΔH is large relative to the other components of ΔE, then $\Delta E \simeq \Delta H$. This means that we could estimate the average size of the multimers (n) formed in

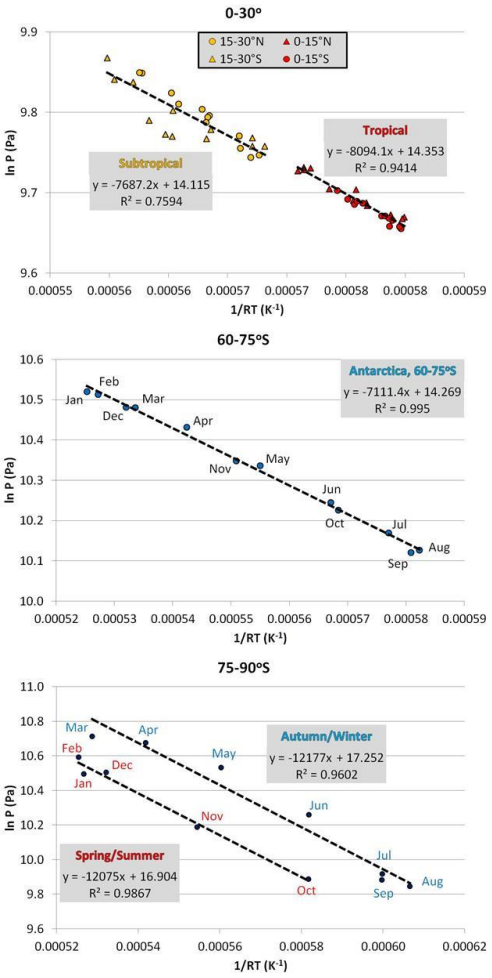

Figure 8: *Plots of* $\ln P$ *against* $\frac{1}{RT}$ *for some of the latitude zones that show clear linear behaviour. In the top panel, the two* $0-15°$ *zones and the two* $15-30°$ *zones are plotted. In the middle panel, the* $60-75°S$ *zone is plotted. For the bottom panel, the* $75-90°S$ *data is split into two linear components, October to February and March to September.*

Zone	ΔE	**mean T**	**mean** n
0-15°N/S	8094 J mol^{-1}	209 K	4.44
15-30°N/S	7687 J mol^{-1}	214 K	4.21
60-75°S	7111 J mol^{-1}	215 K	3.99
75-90°S (Oct-Feb)	12075 J mol^{-1}	221 K	5.71
75-90°S (Mar-Sep)	12177 J mol^{-1}	210 K	5.98

Table 3: *Average size of multimers implied by the plots for the four regions considered in Figure 8, if* $\Delta E \simeq \Delta H$.

those regions by substituting our values for ΔH and the mean temperature for the region into Equation 15. In Table 3, we have estimated the mean values of n for each of these regions, by taking this assumption.

Our calculations in Table 3 suggest that $n \simeq 4$ in the low latitude zones and also 60-75°S, i.e., that the multimers are mostly tetramers. However, for the 75-90°S zone, $n \simeq 6$, suggesting the multimers are mostly hexamers. Perhaps, the multimers are a mixture of different sizes, but the average value is $n \simeq 4$ for the 0-30° and the 60-75°S zones, while the average value is $n \simeq 6$ for the 75-90°S zone.

If we consider the other zones, the relationship between P and T is not very linear, and so we cannot calculate ΔE from the slope. Indeed, for some of the mid-latitude zones, the seasonal variation is almost circular (Figure 7). However, interestingly, for the extra-tropical Northern Hemisphere (30-90°N), there seems to be a linear relationship between P and T with latitude for each of the summer months.

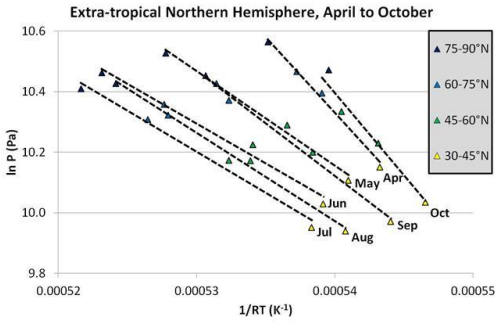

Figure 9: *Plots of* $\ln P$ *against* $\frac{1}{RT}$ *by month for the four extra-tropical Northern Hemisphere latitude zones, i.e.,* $30-90°N$ *from April to October.*

Figure 9 plots $\ln P$ against $\frac{1}{RT}$ for the four extra-tropical Northern Hemisphere zones for each of the months April to October. The values of ΔE implied by these linear fits are relatively large (26295-54218 J mol^{-1}), and if we again assume that $\Delta E \simeq \Delta H$, then this suggests that the average size of the multimers in the extra-tropical Northern Hemisphere summer is $n \simeq$ 10-12, and that this increases to ~ 20 in the spring/autumn - see Table 4.

In our various estimates of n described above, we explicitly assumed that $\Delta E \simeq \Delta H$. However, this assumption need not necessarily hold. If the other components of ΔE become significant, then this would

Month	ΔE	mean T	mean n
April	50006 J mol^{-1}	223 K	19.30
May	31198 J mol^{-1}	225 K	12.44
June	26295 J mol^{-1}	227 K	10.64
July	27193 J mol^{-1}	228 K	10.93
August	29157 J mol^{-1}	226 K	11.67
September	34783 J mol^{-1}	224 K	13.77
October	54218 J mol^{-1}	222 K	20.93

Table 4: *Average size of multimers for the four extra-tropical Northern Hemisphere latitude zones considered in Figure 9, i.e., $30-90°N$, from April to October, if we assume that $\Delta E \simeq \Delta H$.*

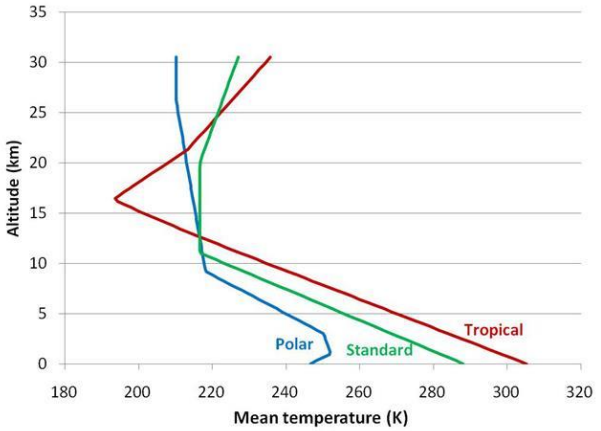

Figure 10: *Polar, standard mid-latitude and tropical altitudinal temperature profiles. Data taken from the US Defense Department's "Non-standard atmospheres" dataset, downloaded from the Public Domain Aeronautical Software website (original source: document MIL-STD-210A). Temperatures were converted from degrees Rankine, and altitudes from feet.*

mean $\Delta H < \Delta E$, and the value of n would be less.

More research is probably required to determine the relative contributions of the other components of ΔE. However, the fact that the ΔE values for the different regions and months in Figures 8 and 9 are comparable to the enthalpies of multimerization for finite values of n supports our theory that multimerization of some of the atmospheric gases could be responsible for the phase transition. It also suggests that the average value of n is not necessarily fixed, but might vary with latitude and/or season.

3 Atmospheric implications of widespread atmospheric multimerization in the tropopause/stratosphere

3.1 New explanation for the altitudinal temperature profiles

Within the troposphere, the mean air temperature tends to decrease with increasing altitude at a *lapse rate* of about -6.5K/km. However, at the tropopause, the lapse rate decreases to about 0K/km, i.e., the temperature "pauses", and in the stratosphere, the lapse rate becomes positive[11].

As can be seen from Figure 10, changes in lapse rate between different atmospheric regions are quite pronounced for all latitudes. Indeed, the troposphere/tropopause/stratosphere regions are typically defined on the basis of their lapse rates. However, the standard explanations for these lapse rate changes are based on the following unjustified assumptions:

1. Aside from changes in water content, the specific heat capacity of the air remains unchanged throughout the troposphere/tropopause/stratosphere regions.

2. The mean molecular weight of the atmospheric gases similarly remains mostly unchanged in the same regions.

3. Most of the atmosphere is only in *local* thermodynamic equilibrium with its surroundings.

If the troposphere/tropopause phase transition involves the formation of multimers, then this would involve changes in both the specific heat capacity and the mean molecular weight of the atmosphere, i.e., it contradicts the first two assumptions.

In Paper I[1], we found that the atmosphere is mostly in *complete* thermodynamic equilibrium with its surroundings over the relatively short distances between the troposphere and stratosphere (i.e., tens of km). This contradicts the third assumption. In Paper III[2], we propose that the atmosphere maintains thermodynamic equilibrium over distances of several thousand km because of the rapid rates of mechanical energy transmission in the atmosphere.

Therefore, new explanations for the atmospheric lapse rates are required. Before we present our explanation, we will briefly summarise the standard explanation for the benefit of readers who are unfamiliar

with it. A more detailed summary can be found in most meteorological textbooks, e.g., Ref. [24].

As altitude (h) increases, so does the gravitational potential energy (mgh - see Equations 17 and 18). If the specific heat capacity of the atmosphere remains constant (as assumed by the standard explanation), then this means that the average thermal energy of the air needs to simultaneously decrease to balance the increase in potential energy. In other words, the mean air temperature decreases with altitude.

Qualitatively, this appears to explain the tropospheric lapse rate[1]. However, as we mentioned above, at the tropopause this negative lapse rate is reduced, and in the stratosphere the lapse rate becomes positive (see Figure 10). In the standard explanation, it is necessary to invoke an external energy source to explain these changes in lapse rates.

In the conventional explanation, it is assumed that this extra energy in the tropopause/stratosphere arises from absorption of solar ultraviolet radiation by ozone in the ozone layer[6, 25], i.e., the *ozone heating hypothesis*. However, this explanation does not hold if the atmosphere is in thermodynamic equilibrium, which we found to be the case in Paper I[1]. If the atmosphere is in thermodynamic equilibrium, then any "extra" energy absorbed by the tropopause/stratosphere would be redistributed amongst the surrounding atmosphere. As we discuss in Paper I, an additional problem with the ozone heating hypothesis is that, during the winter, the polar latitudes receive very little sunlight. Hence, there should not be enough ultraviolet absorption to counteract the negative lapse rate resulting from the increasing potential energy, yet, if anything, the tropopause seems to be *more* pronounced and persistent at the poles than at the equator, since it begins at a much lower altitude (see Figure 10).

Our new explanation for the changes in lapse rates at the tropopause/stratosphere is based on the following assumptions:

1. The troposphere, tropopause and stratosphere are all in thermodynamic equilibrium with each other.

2. The specific heat capacity and mean molecular weight of the atmosphere are *not* necessarily constant.

[1]Although we note that the tropospheric lapse rate predicted by this approach is -9.8K/km, which is more rapid than the experimentally-observed rate of -6.5K/km.

If the troposphere/tropopause phase transition involves the formation of multimers, then the phase transition would cause the average molecular weight of the air to increase. Similarly, the specific heat capacity of the air would change, since the different multimers would have different degrees of freedom (see Table 2), and hence specific heat capacities. As a result, the distribution of energy between the thermal, internal and potential components of the atmospheric molecules will change at the phase transition.

In general, the specific heat capacity of molecules decreases with increasing molecular weight. Hence, as the average molecular weight of the air increases, internal energy is converted into thermal energy, i.e., the average temperature of the air increases. At thermodynamic equilibrium, the atmospheric temperature is therefore a function of *both* the potential energy and the internal energy of the air molecules.

At the tropopause, the lapse rate is close to zero. This suggests that the decrease in temperature with altitude is exactly balanced by the reduction in the average internal energy from the formation of multimers. In the stratosphere, the lapse rate becomes positive. This suggests that the thermal energy increase from the reduction in the average internal energy is greater than the thermal energy decrease from the increasing potential energy.

As discussed in Paper I[1], or as can be seen from Figure 1, the phase transition occurs at the tropopause/troposphere boundary, and not at the tropopause/stratosphere boundary. In other words, there does not seem to be a second phase transition between the tropopause and stratosphere. Hence, the different lapse rates between the tropopause and the stratosphere probably involve a continuous transition. This transition could involve a continuous increase in the fraction of the air molecules which form multimers. Another possibility is that the fraction remains the same, but the average size of the multimers (i.e., n) increases. Both factors might be involved.

3.2 The outgoing terrestrial radiation spectra

If the tropopause phase transition involves the formation of multimers, then this also has implications for some specific features of the Earth's outgoing microwave and infra-red spectra. In this section, we will discuss these features and our explanations for them. However, since our findings in this series of companion papers (this paper along with Papers I[1]

and III[2]) suggest fundamental flaws in the conventional explanations for the Earth's outgoing radiation (*"outgoing terrestrial radiation"*) spectra, we will also use this section to provide our explanations for the general features of the outgoing terrestrial radiation.

The conventional explanations for the outgoing terrestrial radiation spectra are typically described within the framework of the greenhouse effect theory. As we mentioned in Section 1, the greenhouse effect theory relies on the assumption that the air in the troposphere/tropopause/stratosphere regions is only in *local* thermodynamic equilibrium. Essentially, the theory assumes that, over very short distance (e.g., a few metres), the air molecules remain in thermodynamic equilibrium with each other through conduction and convection. But, over longer distances, it is assumed that this equilibrium breaks down, i.e., neighbouring "parcels" of air are thermodynamically isolated from each other. As a result, it is assumed that, if a given parcel of air absorbs or emits more radiation than its neighbours, the total energy of that parcel will change relative to its neighbours. This leads to the assumption that the distribution of energy throughout the atmosphere is predominantly controlled by radiative processes. Pierrehumbert, 2011[3] offers a concise summary of this local thermodynamic equilibrium-based framework.

However, in Paper I[1], we found that, for a given latitude/longitude, the troposphere/tropopause/stratosphere regions are essentially in thermodynamic equilibrium with each other. For this reason, a replacement framework for describing the outgoing radiation spectra is required.

Before we discuss our framework, there are a number of known results and observations in the literature which we believe are important to note. But, the reader should note that many of the references we will cite in this section explicitly or implicitly make the assumption of local thermodynamic equilibrium to explain their results and/or observations. Clearly, there are different ways in which the following results/observations can be individually explained. Our goal in this section will be to provide satisfactory explanations which are *also* consistent with our finding that the troposphere/tropopause/stratosphere regions are in thermodynamic equilibrium. This is important, because the conventional explanation for the outgoing terrestrial radiation does not do so.

A reasonable starting assumption to make is that the total amount of incoming solar radiation that reaches the Earth system (surface + atmosphere) roughly balances the total amount of outgoing terrestrial radiation. This assumption of *radiative balance* is quite common in analyses of the Earth's energy budget, e.g., Kiehl & Trenberth, 1997[26], and we will adopt it here. We do acknowledge that some researchers have considered the possibility that the Earth might have a radiative imbalance, e.g., Trenberth et al., 2009[27]. However, if such an imbalance were to be significant and continuous, it would probably lead to a very rapid cooling or heating of the Earth system, which seems unlikely.

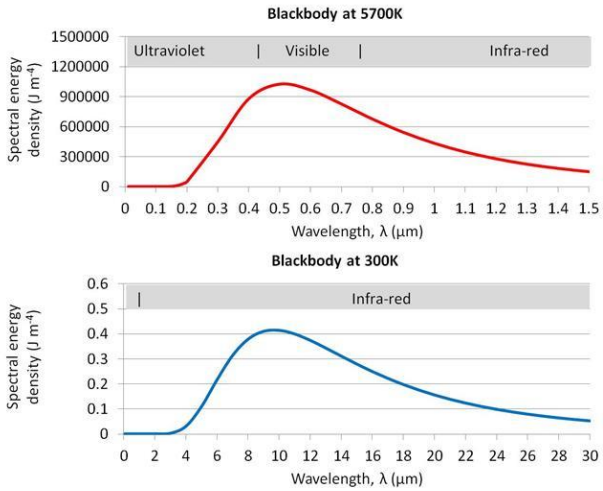

Figure 11: *Theoretical distribution of the radiation emitted by a blackbody at a temperature of (top) 5700K, i.e. the approximate surface temperature of the Sun and (b) 300K, i.e the approximate surface temperature of the Earth. Note that the axis ranges are different for both spectra.*

Because of the high temperature of the sun, the incoming solar radiation is mostly in the form of high frequency *"shortwave radiation"*, i.e., ultraviolet/visible and shortwave infra-red radiation - see Figure 11. Some of this shortwave radiation is reflected back into space, without being absorbed, by various reflective processes, which are collectively referred to as *"albedo"*[2] processes. Most estimates suggest that about one third of the incoming solar radiation is reflected by albedo processes[26].

To maintain radiative balance, the Earth must emit the same amount of energy to space that it absorbs. However, because the surface of the Earth is much cooler than that of the sun, this outgoing terrestrial

[2]After the Latin for "white", *albus*, since white objects reflect most visible light.

radiation is mostly in the form of low frequency *"long-wave radiation"*, i.e., longwave infra-red radiation - see Figure 11. The Earth is also predicted to have some microwave emissions, but the total energy of these emissions is small relative to the infra-red emissions.

Satellite observations suggest that the total incoming solar radiation at the top of the atmosphere is ~ 340 W/m^2, when averaged over the entire surface area of the planet[3]. Of the outgoing terrestrial radiation, ~ 100 W/m^2 is reflected solar radiation ("outgoing shortwave terrestrial radiation"). The remaining ~ 240 W/m^2 accounts for the "outgoing longwave terrestrial radiation". See e.g., Ramanathan et al., 1989[28] or Kiehl & Trenberth, 1997[26], for more precise estimates of these three values.

In this section, we will be mostly considering the latter component, i.e., the outgoing longwave terrestrial radiation. We can subdivide this further into the radiation emitted from the Earth's surface and the radiation emitted from the atmosphere.

As a first approximation, the spectrum of the outgoing terrestrial radiation from the surface can be described as being similar to that of a black-body with the temperature of the surface, i.e., something roughly like the bottom panel of Figure 11. However, since the atmosphere lies between the surface and space, the actual outgoing terrestrial radiation, as seen from the top of the atmosphere, will be modified by the absorption and emission of radiation by the atmosphere.

In the 19th century, Tyndall, 1861[29] found that the two bulk atmospheric gases - N_2 and O_2 - did not directly interact with "heat" (i.e., infra-red radiation). Although the third bulk atmospheric gas (Ar) had not been discovered at the time, it also does not directly interact with infra-red radiation. However, he found that water vapour and some of the trace atmospheric gases were capable of absorbing infra-red radiation. It is now known that gases which absorb radiation at a given frequency can also emit radiation at that frequency. Essentially, Tyndall had identified that only some of the atmospheric gases are *infra-red active*, i.e., can directly absorb and emit infra-red radiation.

The infra-red active gases are popularly referred to as "greenhouse gases", because of their relevance to the greenhouse effect theory. However, we will favour the term infra-red active gases, since it better describes their spectroscopic properties.

In the Earth's atmosphere, the three most abundant infra-red active gases are water vapour (H_2O), carbon dioxide (CO_2) and ozone (O_3). This means that most of the atmosphere's absorption and emission of the outgoing longwave terrestrial radiation occurs through these trace gases.

The infra-red spectra of H_2O, CO_2 and O_3 each have several active bands in the range of infra-red radiation that the surface is expected to emit. As a result, much of the radiation leaving the Earth's surface is absorbed by the atmosphere. There are a few relatively narrow bands of infra-red radiation in this range which do not include an active band from any of the greenhouse gases, e.g., $3.4 - 4.0\mu$ or $8.0 - 13\mu$. Since the atmosphere is *relatively* transparent in these non-active bands, they are sometimes referred to as the "atmospheric window" bands. However, even within the atmospheric window, the atmosphere still absorbs some radiation.

For instance, when Gebbie et al., 1951 analysed the atmospheric transmission across several miles of sea in the range $1 - 14\mu$ they were unable to find any completely transparent regions[30]. Even for the most transparent bands, only 80-90% of the radiation was transmitted per sea mile. In terms of air mass, a horizontal column of air one sea mile long at sea level is roughly equivalent to a vertical column of nearly a quarter of the atmosphere[4]. So, at those transmission rates, only about 1/3 to 2/3 of the radiation passing through the "window" would leave the atmosphere without being absorbed[5].

From this we can conclude that most of the outgoing longwave terrestrial radiation from the Earth's surface is absorbed by the atmosphere before it has the chance to leave the atmosphere. In other words, although there is a small component of direct emission to space from the surface through "the window", most of the outgoing longwave terrestrial radiation is

[3] This is exactly 1/4 of the Total Solar Irradiance shown in Figure 5, since the surface area of the Earth is $4\pi r^2$, where r = radius of the Earth, yet the surface area in sunlight is only πr^2.

[4] 1 sea mile = 1852m and the density of air at sea level = 1.293kg m^{-3}. Therefore, the weight of air in a horizontal column 1 sea mile long = $1852 \times 1.293 \times 9.81 = 23490$ N m^{-2}=23490 Pa. As the weight of air above the surface is 100000 Pa under standard conditions, the mass of air in a vertical column above the surface is equivalent to $\frac{100000}{23490} = 4.257$ times the mass of air in a horizontal column 1 sea mile long, at sea level.

[5] Horizontal transmission of 80%/sea mile is equivalent to a vertical transmission through the entire atmosphere of roughly $0.8^4 = 0.41 = 41\%$, while a horizontal transmission of 90%/sea mile corresponds to a vertical transmission of $0.9^4 = 0.66 = 66\%$.

emitted from the atmosphere itself.

With increasing altitude, the atmospheric density decreases. As the atmospheric density decreases, so will its infra-red opacity. So, with increasing altitude, an increasing amount of the infra-red radiation which is emitted by the atmospheric gases will escape to space without being re-absorbed by the surrounding gases. In the conventional explanation, the region of the atmosphere at which most of this occurs is the tropopause/stratosphere[3]. This seems reasonable to us, and we agree that much of the outgoing longwave radiation is probably emitted in this manner. The infra-red radiation emitted from these regions should mostly be in the infra-red active bands of the main emitting gases there, i.e., CO_2, H_2O and O_3.

When the Mars Global Surveyor carried out its analysis of the outgoing terrestrial radiation on November 24, 1996 (from a distance of 4.7 million km), it detected strong spectral features from the three main infra-red active gases, which appeared to have originated from the tropopause/stratosphere regions. It also detected some infra-red radiation in the "window" bands, which appeared to have been emitted from the surface[31]. So, it appears that many of the features of the outgoing longwave terrestrial radiation can be explained in terms of the two mechanisms described above, i.e., (1) surface emission through the "atmospheric window" and (2) atmospheric emission by the infra-red active gases in the tropopause/stratosphere regions.

However, there are at least two other mechanisms which should also contribute substantially to how the outgoing longwave radiation is emitted. One of these mechanisms is through cloud formation (mostly in the troposphere) and the other is through the formation of oxygen multimers in the tropopause/stratosphere regions.

Clouds are known to absorb, emit and reflect infra-red radiation over a wide range of wavelengths - see e.g., Refs. [28, 32, 33]. One factor is that clouds comprise liquid or solid water, both of which have stronger infra-red spectra than water vapour. Another factor is that the size of the cloud droplets can become large enough to cause Mie scattering[34]. A third factor is worth some discussion, as it has similarities to our proposed mechanism for infra-red emission by multimer formation.

In order for a cloud to form, water vapour molecules must condense to form either liquid droplets (at warmer temperatures) or ice crystals (at colder temperatures). This means that, when the water vapour molecules collide with each other, some of the collisions are *inelastic*, i.e., when two molecules collide, they stick together. The same process is also involved in multimer formation.

In order for an inelastic collision to occur, the molecules must gain or lose energy. In our two cases (cloud formation and multimer formation), they must lose energy. Typically, this is by the emission of electromagnetic radiation. So, after collision, the excited molecules must have a mechanism for emitting electromagnetic radiation with an energy comparable to the extra energy from the collision. Otherwise, the collision will be elastic, and the molecules will separate again.

As we mentioned above, water vapour molecules can emit infra-red radiation. They can also emit microwave radiation ($\sim$ 22GHz). Hence, when water vapour molecules collide, they can coalesce to form clouds by emitting either infra-red or microwave radiation. If the cloud is at a high enough altitude, some of this radiation may be transmitted out to space without being reabsorbed by the atmosphere. However, much of the radiation will be absorbed by the water molecules in the surrounding air, since they are capable of absorbing radiation at the same wavelengths. This will cause the water molecules to heat up, and through elastic collisions with other nearby air molecules, will cause the surrounding air molecules to heat up.

As we discussed above, we have found that the air in the troposphere/tropopause/stratosphere is mostly in thermodynamic equilibrium. So, this extra thermal energy will be rapidly distributed throughout the atmosphere. However, *before* the energy is distributed, *some* of the excited molecules may emit some radiation, if they have a mechanism for doing so, e.g., the infra-red active gases. Again, if the cloud is at a high enough altitude, some of this radiation may be transmitted out to space, and therefore contribute to the outgoing terrestrial radiation.

Hence, cloud formation can contribute to the outgoing terrestrial radiation both directly (through the coalescing molecules) and indirectly (through excitation of the surrounding air molecules).

Since N_2 and O_2 are not infra-red active gases, it might initially appear that they would be incapable of forming multimers under atmospheric conditions, since they are not able to undergo inelastic collisions by infra-red emission. However, because diatomic oxygen is a paramagnetic molecule, it is able to absorb and emit microwave radiation[35] at a frequency

of $\sim$ 60GHz. Hence, two or more oxygen molecules can coalesce together to form oxygen multimers, by emitting microwave radiation,

$$nO_2 \Longleftrightarrow (O_2)_n + h\nu \text{ (60 GHz)} \tag{20}$$

Although nitrogen molecules cannot *directly* coalesce together since they are diamagnetic, once an oxygen multimer is formed, it may be that a nitrogen molecule could displace one of the oxygen monomers in the multimer through collision. In other words, there is a potential mechanism for the formation of nitrogen/oxygen mixed multimers, i.e.,

$$(O_2)_n + N_2 \Longleftrightarrow (O_2)_{n-1}(N_2) + O_2 \tag{21}$$

This step could potentially be repeated until all of the oxygen monomers have been replaced with nitrogen monomers, to yield a nitrogen multimer, i.e.,

$$(N_2)_{n-1}(O_2) + N_2 \Longleftrightarrow (N_2)_n + O_2 \tag{22}$$

So, through the emission of microwave radiation, there is indeed a mechanism for the formation of the oxygen, nitrogen and mixed multimers which we discussed in Section 2. What are the implications of this for the outgoing terrestrial radiation?

First, some of the emitted microwave radiation may be transmitted to space, and thereby directly contribute to the outgoing terrestrial radiation. In this context, it is worth noting that when Spencer & Christy, 1990 were constructing a satellite based atmospheric temperature dataset using measurements from a series of microwave sounding units at frequencies near the 60GHz band, they were unable to include data from the channel centred on the tropopause region (Channel 3), due to an increase in microwave emissions[4]. We suspect that this is due to the formation of oxygen multimers at the phase transition.

Having said this, because oxygen can absorb as well as emit microwave radiation at this frequency, we suspect that most of the emitted microwave radiation is reabsorbed by the surrounding oxygen molecules. These excited oxygen molecules could then start to heat the other air molecules through collisions. As with the cloud formation, if any of the infra-red active gases are excited by this process, some of them may emit infra-red radiation before thermodynamic equilibrium is re-established.

As an aside, Spencer & Christy, 1990 also were unable to use the microwave channel centred on the lower troposphere (Channel 1), due to emissions from clouds (as well as the surface)[4]. This could be due to microwave emission from some of the oxygen molecules in the excited air molecules near the site of the coalescing cloud.

At any rate, we can see that multimer formation can *indirectly* contribute to the outgoing infra-red terrestrial radiation through the excitation of the surrounding infra-red active gases. Since multimer formation occurs in the same regions that we expect the general atmospheric emission to space to take place (i.e., the tropopause/stratosphere), and both mechanisms involve emission through infra-red active gases, it may be difficult to determine the relative contributions of the two mechanisms.

To summarise, we have identified four different mechanisms which contribute to the outgoing longwave terrestrial radiation:

1. Some infra-red radiation will be emitted directly from the surface through the "atmospheric window". We would also expect some surface radiation to escape to space from outside of the "window" bands, but the amount from these less transparent bands will be substantially reduced.

2. More infra-red radiation will be emitted from the atmosphere itself. This radiation is emitted by the infra-red active gases, e.g., H_2O, CO_2, O_3. The emissions which leave the atmosphere will mostly be from the middle parts of the atmosphere, i.e., the tropopause/stratosphere, since the troposphere is too opaque and the density of the upper atmosphere is much lower.

3. Cloud formation will directly and indirectly lead to infra-red emissions, some of which will leave the atmosphere.

4. The formation of oxygen multimers at the tropopause will indirectly lead to infra-red emissions, some of which will leave the atmosphere.

Described in this manner, mechanisms 1-3 are very similar to the conventional explanation for the outgoing terrestrial longwave radiation spectrum. Indeed, initially they might appear identical. However, there is a key difference between our explanation and the conventional explanation. At no stage during our explanation did we invoke the assumption that the troposphere/tropopause/stratosphere are only in *local* thermodynamic equilibrium, whereas the conventional explanation relies heavily on this assumption.

Hence, our explanation *is* compatible with our observation from Paper I that these regions are in thermodynamic equilibrium.

In the conventional explanation, the altitudinal temperature profile of the atmosphere is intrinsically tied to the shape and distribution of the outgoing terrestrial spectrum. Hence, when Harries et al., 2001 found that this spectrum had changed from 1970 to 1997, they concluded (in our opinion, incorrectly) that this *"provide[d] direct experimental evidence for a significant increase in the Earth's greenhouse effect"*.

In our explanation, the altitudinal temperature profile is a consequence of the thermodynamic properties of the atmosphere, as we discussed in Section 3.1 and Paper I[1]. The shape and distribution of the outgoing terrestrial spectrum does *not* have to be tied to this temperature profile. Instead, it is mostly related to the atmospheric composition and the amount of incoming solar radiation. In other words, altering the relative concentrations of the infra-red active gases ("greenhouse gases") in the atmosphere should alter the shape (or "colour") of the outgoing terrestrial radiation spectra, but should not in itself alter the altitudinal temperature profile within the atmosphere. We note that this has implications for astronomers who are attempting to estimate the altitudinal temperature profiles of other planets using the infra-red spectra of the planets.

With regard to the outgoing microwave radiation, we agree with Spencer & Christy, 1990[4] that the microwave emissions from the troposphere are related to (a) cloud formation and (b) surface emissions. However, we disagree with their explanation that the microwave emissions from the tropopause are a result of the altitudinal temperature profile. Instead we believe that they are due to the formation of oxygen multimers. We do not know exactly how the microwave emissions from the tropopause are distributed, or what their intensities are, since Spencer & Christy, 1990 only briefly refer to them. But, we suspect that a careful examination of their "Channel 3" dataset would provide useful insights into the multimerization of the atmospheric gases at the tropopause. We believe this could be a valuable future research direction for the study of the phase transition.

3.3 Alternative mechanism for ozone formation in the ozone layer

In the Earth's atmosphere, ozone (O_3) is just a trace gas which only comprises a few parts per billion by volume of the atmosphere. In this context, ozone concentrations are quite high in the stratosphere, even though ozone still only accounts for a few parts per million by volume of the stratosphere. For this reason, the region of the stratosphere with relatively high ozone concentrations is often referred to as the *"ozone layer"* (altitudes of roughly ~20-45 km).

In the early 20th century, several researchers attempted to explain the existence of this ozone layer, and the related question of how the stratospheric ozone was generated. Chapman, 1930[6] suggested that the stratospheric ozone was generated in a two step process and destroyed by a third step. This is now known as the "Chapman mechanism".

Although additional mechanisms for the depletion of ozone are now included, the Chapman mechanism is widely assumed to be the primary mechanism for stratospheric ozone generation, e.g., see reviews by Rowland, 2006[36] and Solomon, 1999[37]. However, although some researchers have considered the possibility that temporary, collision-induced oxygen dimers might play a role in ozone formation[38], the role of oxygen multimers in ozone formation seems to have been overlooked until now. In this section, we will discuss a multimer-based alternative to the Chapman mechanism. Before we do so, it may be helpful to briefly review the Chapman mechanism, and the conventional explanations for other aspects of the stratospheric ozone layer.

Essentially the Chapman mechanism proposes that, in the stratosphere, the incoming ultraviolet solar radiation photolyses some of the diatomic oxygen molecules to produce reactive atomic oxygen radicals ($O^\bullet$),

$$O_2 + h\nu(< 242\text{nm}) \Longrightarrow 2O^\bullet \qquad (23)$$

In a second step, these oxygen radicals react with other oxygen molecules, forming ozone (and also releasing the thermal energy which forms the basis for the ozone heating explanation for the stratospheric temperature lapse rates discussed in Section 3.1),

$$O^\bullet + O_2 \Longrightarrow O_3 + \text{Energy} \qquad (24)$$

Chapman, 1930 also proposed that this ozone could be broken down again by a further ultraviolet photolysis step,

$$O_3 + h\nu(< 242\text{nm}) \Longrightarrow O^\bullet + O_2 \qquad (25)$$

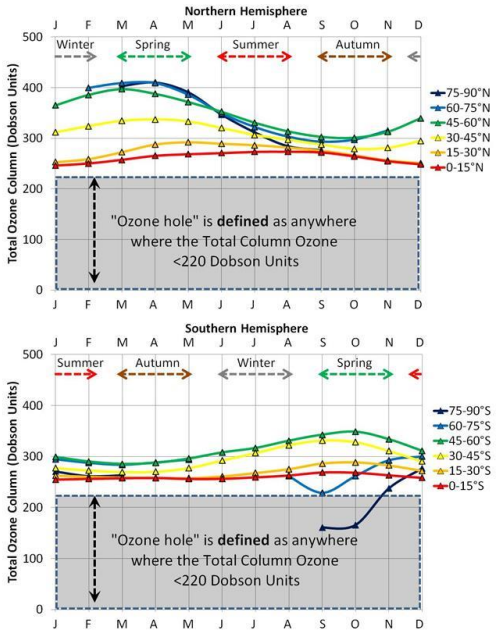

Figure 12: *Mean total column ozone concentrations (in Dobson Units) by month for each of the latitudinal zones, over the 1996-2005 period.*

If the Chapman mechanism was the main mechanism for ozone formation, then it would be expected that ozone concentrations would be greatest at the equator, where the most sunlight arrives, and would decrease with latitude. However, as can be seen from Figure 12, aside from the Antarctic region, this is the opposite of what is observed.

Also, ozone concentrations should peak in the summer (when incoming solar radiation is greatest) and reach a minimum during the winter. However, it can be seen from Figure 12 that the actual maximum concentrations tend to occur during the spring, and reach a minimum during the autumn (again, the Antarctic is an exception, with minimum concentrations during the spring).

In order to explain these apparent contradictions, the standard theory proposes that, while ozone generation is greatest at the equator, once formed, it is then *slowly* transported downwards towards the poles in the stratosphere over the course of several months. This proposed equator-to-poles stratospheric atmospheric circulation is referred to as the "Brewer-Dobson circulation" after Brewer, 1949[39] and Dobson, 1956[40]. The lower altitude of the ozone at higher latitudes is also explained by the same circulation, in that the air mass is supposed to sink as it travels towards the poles.

An additional problem with the Chapman mechanism is that model predictions based on it substantially underestimate the concentrations of ozone in the upper stratosphere ($>$ 35km), compared to satellite observations[41]. Various suggestions have been made to account for this "ozone deficit problem", although so far they have only partially accounted for the problem, e.g., Miller et al., 1994[38].

During the 1960s and 1970s, several researchers suggested that there were additional mechanisms for the depletion of stratospheric ozone, as well as Chapman's Equation 25. Typically, these mechanisms involve the catalytic depletion of ozone by various reactive radical species, other than $O^{\bullet}$. A large number of such mechanisms have now been proposed, but they are generally grouped together on the basis of the type of radical species involved. Hence, there are now mechanisms involving "odd hydrogen" ($H^{\bullet}$,$OH^{\bullet}$, $HO_2^{\bullet}$), "odd nitrogen" ($NO^{\bullet}$, $NO_2^{\bullet}$) and "odd chlorine" ($Cl^{\bullet}$, $ClO^{\bullet}$). See Refs. [36, 37, 41] for reviews of these different mechanisms.

The conventional explanations for stratospheric ozone concentrations assume that ozone formation is quite slow, e.g., it is assumed to take several months for the "tropically-formed" ozone to reach the poles. Hence, a number of researchers became concerned that human activity could be causing an increase in the concentration of various molecules in the stratosphere which might significantly decrease ozone concentrations in the ozone layer through one of the catalytic ozone depletion mechanisms.

In particular, there was concern that the increasing use of man-made chlorofluorocarbon (or "CFC", for short) molecules was leading to an increase in the concentration of "odd chlorine" radicals in the stratosphere. When measurements of stratospheric ozone concentrations revealed a general downward trend during the 1980s-1990s, particularly for the Antarctic regions, this convinced many that the use of CFCs was seriously affecting ozone concentrations in the ozone layer[36, 37] (although some researchers disagreed, e.g., Singer, 1993[42]). As a result, there has been an international agreement, through the "Montreal Protocol" (and its subsequent revisions) to rapidly phase-out the production of CFCs. Salby et al., 2012 suggest that there has been a gradual increase in Antarctic ozone concentrations since the 1990s[43].

However, if oxygen multimers comprise an appreciable fraction of the stratospheric atmosphere (as we

proposed in Section 2), then this suggests an alternative mechanism for the formation of stratospheric ozone,

$$(O_2)_n + h\nu(\text{ultraviolet}) \Longrightarrow O_{2n-3} + O_3 \qquad (26)$$

If $n = 2$, i.e., a dimer, then $O_{2n-3} = O^\bullet$. If $n = 3$, i.e., a trimer, then Equation 26 could involve the splitting of one trimer molecule into two ozone molecules. For higher values of n, the O_{2n-3} "molecule" may in fact comprise several different oxygen allotropes, depending on n, the relative stability of the various allotropes, etc. But, for our purposes, it is sufficient here to note that the formation of ozone could involve the *uni-molecular* splitting of an oxygen multimer by ultraviolet photolysis[6].

In contrast to our proposed mechanism, the Chapman mechanism for ozone formation (Equation 24) is a *bi-molecular* reaction, which requires the collision of two molecules before reaction can take place. Indeed, since the energy released from the reaction must be absorbed by collision with a third molecule, it is often described as a tri-molecular reaction,

$$O^\bullet + O_2 + M \Longleftrightarrow O_3 + M \qquad (27)$$

Where M is an arbitrary molecule which absorbs the excess energy of ozone formation through an inelastic collision.

In addition, our mechanism just involves a one-step process (photolysis of multimers) to generate ozone[7], while the Chapman mechanism involves two steps. For both of these reasons, we would expect our mechanism to be much faster (one-step, first order reaction) than the Chapman mechanism (two-step, second order reaction).

As we discussed in Section 2.1, the average phase transition conditions vary with season and latitude. So, this could also explain the seasonal and regional variability in stratospheric ozone concentrations. Hence, let us compare the mean monthly stratospheric ozone concentrations to the corresponding phase transition conditions for each of the latitudinal zones.

To estimate the variability of stratospheric ozone with season and latitude, we used National Aeronautics and Space Administration (NASA)'s Total Ozone Mapping Spectrometer (TOMS) measurements from the Earth Probe satellite which operated from July 1996 until December 2006. These measurements are estimates of the daily "Total Column Ozone" at a given latitude and longitude, in Dobson units (100 Dobson units corresponds to a layer of ozone gas that would be 1mm thick if compressed to standard temperature and pressure). Since the estimates are determined from reflected solar radiation (ultraviolet), they cannot be made during the polar winters, as it is too dark. However, aside from that, the estimates can provide global coverage over the entire year.

We downloaded all the available monthly averaged measurements from the satellite (August 1996-November 2005) from ftp://toms.gsfc.nasa.gov/pub/eptoms/data/zonal_means/ozone/. The TOMS data was zonally averaged into 5° latitude bands. So, for comparison with our zonal mean climatologies for the phase transition, we averaged together the three 5° latitude bands corresponding to each of the 15° latitude bands in Figure 3. We then calculated the equivalent ozone climatologies by averaging all measurements for a given calendar month.

Zone	r	**Total Column Ozone (D. U.)**	**Pressure (Pa)**
$75-90°$N	0.766	276-410	31400-38700
$60-75°$N	0.749	293-409	30000-35100
$45-60°$N	0.773	301-397	26200-32200
$30-45°$N	0.557	279-337	20700-26300
$15-30°$N	0.480	251-292	17300-19300
$0-15°$N	0.917	246-274	15800-16800
$0-15°$S	0.658	255-269	15600-16400
$15-30°$S	0.849	258-289	17100-18900
$30-45°$S	0.739	270-331	20200-26300
$45-60°$S	0.718	286-349	26500-31300
$60-75°$S	0.812	229-300	24800-37000
$75-90°$S	0.895	**161**-277	18900-44900

Table 5: *The range of stratospheric ozone concentrations ("Total Column Ozone") for each of the latitudinal zones, along with the range of pressures at which the phase transition occurs for those zones ("Pressure"). The monthly correlations between Total Column Ozone and phase transition pressure for each of the zones are also listed ("r").*

In Figure 13 (next page), we compare the mean monthly zonal ozone concentrations (over the 1996-2005 period) to the corresponding mean phase transition pressure. The ranges of values are also listed in Table 5.

[6] The splitting could also be thermally driven, e.g., through high energy molecular collisions. However, since ultraviolet solar radiation is absorbed in the ozone layer, we assume that at least some of the ozone formation is by ultraviolet photolysis.

[7] Although, the photolysis may also lead to further reactions involving the remaining part of the multimer, depending on n.

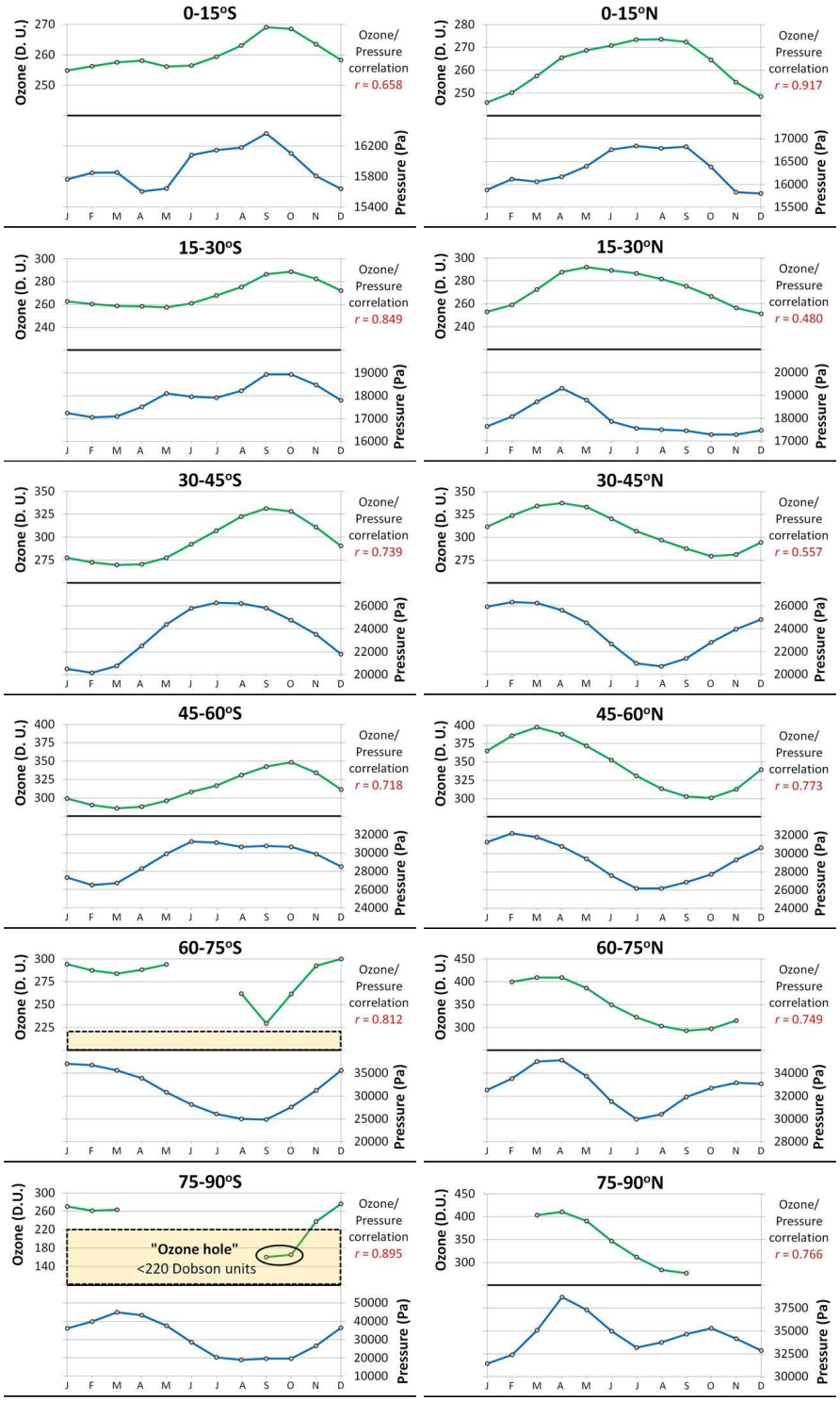

Figure 13: *Mean ozone concentrations ("Total Column Ozone"), in Dobson units (D.U.) by month for each of the zones in Figure 3, compared to the corresponding mean pressure of the phase transition. An "ozone hole" is defined as any region with a Total Column Ozone of less than 220 Dobson units. Note that the y-axis ranges vary for each of the plots.*

The two parameters seem to be highly correlated; for 9 of the 12 zones, $r > 0.7$[8]. Even for the least correlated zone ($15 - 30°N$), there is still a positive correlation of $r = 0.480$.

Why would stratospheric ozone concentrations be correlated to the phase transition pressure? If the phase transition occurs at a high pressure, then this means that multimers should begin forming at a low altitude. Because current weather balloons only reach an altitude of $\sim 30 - 35$km, our analysis of the phase transition only covers the region up to the mid-stratosphere. So, our current analysis does not indicate the upper altitudes for multimer formation. However, it seems reasonable to assume that, if multimers start forming at a lower altitude, then the range of altitudes over which multimers exist increases. Therefore, if ozone is formed from oxygen multimers (Equation 26), then we would expect stratospheric ozone concentrations to generally increase as the phase transition pressure increases, as is observed in Figure 13.

One potential problem with this explanation for the correlation is that, if multimer formation requires the same short wavelength ultraviolet radiation that the Chapman mechanism does, then most of the shorter wavelength ultraviolet radiation would be absorbed at the higher altitudes. Hence, there would not be enough radiation to photolyse the multimers at the lower altitudes. Indeed, we know that most of the incoming ultraviolet radiation from the sun is absorbed by the ozone layer, before reaching the ground, particularly for the shortest wavelengths. However, perhaps the range of wavelengths which can photolyse multimers to generate ozone is different from the range of wavelengths required by the Chapman mechanism.

If so, then even after all of the shorter wavelength ultraviolet solar radiation has been absorbed by the upper stratosphere, there may still be wavelengths which can induce photolysis of the multimers. It might be possible to test this hypothesis by comparing ground-level measurements of the solar radiation spectrum to estimates of the total column ozone at the time of measurement. However, it must be remembered that the traditional method for measuring total column ozone involves comparing the relative intensities of different ultraviolet bands at ground level, so care should be taken in making such comparisons.

[8]The Pearson product-moment correlation coefficient, r, varies from +1 (perfectly correlated) to 0 (non-correlated) to -1 (perfectly anti-correlated).

A second potential problem is that the pressure of the phase transition is not perfectly correlated with ozone concentrations, e.g., for $15 - 30°N$, r is only 0.480. However, this is not surprising. First, pressure is not the only factor which determines the phase transition. For instance, we saw from Figure 4 that the relationship between the temperature and pressure of the phase transition is sometimes complex. Second, it is likely that the efficiency of ozone formation from multimers depends on n, the size of the multimers. In Section 2.3, we found that the average size of the multimers is different for different zones, and possibly seasons.

For these reasons, we believe that multimer photolysis is indeed a significant mechanism for ozone formation in the stratosphere. Moreover, the strong correlation between ozone concentration and the phase transition conditions indicates that the mean stratospheric ozone concentration at a given location and time of year is mostly determined by phase transition conditions. This has some important consequences.

First, it suggests that stratospheric ozone is *mostly* formed by the photolysis of oxygen multimers, and not by the Chapman mechanism (as had been previously assumed). According to the conventional paradigm, ozone is mainly produced near the equator, but then is transported towards the poles by slow stratospheric circulation patterns, i.e., the proposed Brewer-Dobson circulation. Indeed, in this paradigm, it is widely assumed that ozone concentrations can actually be used as a *"tracer"* for mapping stratospheric circulation patterns[44, 45].

Several studies have reported correlations between polar ozone concentrations and different meteorological parameters, such as stratospheric temperatures, e.g., Refs. [43, 44, 46, 47]. Until now, these have generally been assumed to be *"causative correlations"*, i.e., correlations which exist because one parameter directly influences the other. For instance, Leovy et al., 1985[44] and Salby & Callaghan, 2004[46] have suggested that stratospheric warming at the poles alters the stratospheric circulation, and thereby increases the amount of ozone transported from the tropics to the poles. Other studies have suggested that *"polar stratospheric clouds"* lead to ozone depletion, and that stratospheric heating prevents the formation of polar stratospheric clouds, and thereby "reduces ozone depletion" (i.e., increases the polar ozone concentrations), e.g., Salby et al., 2012[43] or Parrondo et al., 2014[47].

However, if our proposed multimer-related mecha-

nism for ozone formation is correct, then ozone is generated and destroyed *in situ*. This would mean that ozone concentrations are *not* a tracer for stratospheric circulation. Indeed, this would remove the main basis for assuming there is a "Brewer-Dobson circulation". We recognise that the Brewer-Dobson circulation is now considered a "textbook" description, e.g., Salby, 1996[48], but maybe our understanding of stratospheric circulation should be revisited. Perhaps more direct experimental methods than using "tracers" are necessary to determine the true stratospheric circulation patterns.

But, in that case, what is the reason for the reported correlations between ozone concentrations and stratospheric temperatures (or other meteorological parameters)? We suggest that the correlations are instead *"commensal correlations"*, i.e., they are not directly related to each other, yet both have a causative correlation to a common factor, in this case the distribution of multimers in the atmosphere.

We saw in Section 3.1 that multimerization alters the altitudinal temperature profile - we discuss this in more detail in Paper I[1]. So, if the multimer distribution changes then this can alter the altitudinal temperature profile, e.g., it could cause stratospheric heating or cooling. Similarly, the multimer distribution influences the amount of ozone generated. Hence, a change in multimer distribution could alter *both* stratospheric temperatures *and* ozone concentrations. In other words, stratospheric temperatures and ozone concentrations might be commensally correlated, without either influencing the other. Revisiting these correlations from this perspective might provide new insights into all three parameters, i.e., multimer distribution, stratospheric temperatures *and* ozone concentrations.

Second, it suggests that the rate of ozone generation is considerably faster than had been previously assumed. This substantially reduces the urgency of the concern over atmospheric CFC concentrations, since the basis for the concern was the belief that ozone generation took several months (or longer). Morover, since the average phase transition conditions change over time (Section 2.1), the average stratospheric ozone concentrations should also change over time. Hence, many of the observed trends in stratospheric ozone concentrations may have been a result of naturally-occurring climatic trends.

There is considerable evidence that average stratospheric ozone concentrations declined during the late 20th century (1980s-1990s), particularly during the Antarctic spring[36, 37]. However, before 1957, systematic ozone measurements were very limited[49], and in those cases where early measurements are available, it is unclear how directly comparable they are to modern measurements[50]. It may be that reliable estimates for earlier ozone concentrations could be inferred from indirect measurements, such as reanalysis of astronomical photographic plates[51]. But, for now, it is difficult to know whether the 1980s-1990s decline in ozone concentrations relative to those during the 1960s-1970s is unusual or not.

In some senses, from a political point-of-view, it might not really matter whether or not CFCs played a role in the 1980s-1990s decline, since the production of CFCs has already been considerably phased-out, through international agreements such as the Montreal Protocol[36]. However, in light of the above findings, it may be worth reassessing the CFC-related explanation for recent ozone trends, from a scientific point-of-view.

Finally, if ozone can be formed by the photolysis of oxygen multimers, it is plausible that the photolysis of nitrogen/oxygen multimer mixtures would similarly lead to the formation of different nitrogen oxides. With this in mind, it is interesting to note that various nitrogen oxides collectively referred to as NO_y are often found to be closely correlated to the presence of O_3 in the stratosphere, e.g., Ref. [52]. It is possible that some of this NO_y is generated by the photolysis of mixed multimers.

3.4 How shifts in the location of the phase change boundary affect weather

Rapid changes in the heights of the phase change boundary in a column of air can alter the atmospheric pressure profile for that column, which in turn can alter the atmospheric pressure profile of the surrounding air. This has important implications for the weather.

The pressure at a given location in an air column depends on the temperature and molar density, i.e., by rearranging Equation 1, we obtain,

$$P = DRT \tag{28}$$

If the phase change boundary decreases in altitude, this means that multimers begin forming at a lower altitude, i.e., it increases the number of multimers. For a given mass of air, increasing the number of multimers decreases the molar density, and hence

the pressure. That is, it creates a partial "vacuum". Driven by this new pressure gradient, the surrounding air will flow in to fill this partial vacuum, reducing the pressure of the surrounding air. See Figure 14 for a schematic representation.

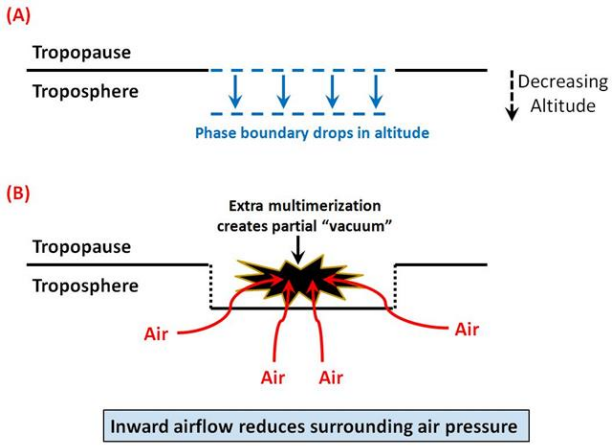

Figure 14: *Schematic depiction of how changes in the location of the phase boundary can lead to low pressure or cyclonic conditions.*

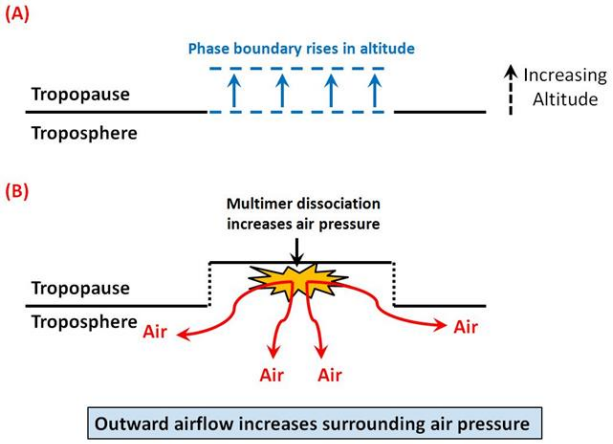

Figure 15: *Schematic depiction of how changes in the location of the phase boundary can lead to high pressure or anti-cyclonic conditions.*

On the other hand, if the phase change boundary increases in altitude, then the reverse scenario applies. The dissociation of multimers into monomers increases the molar density, and hence the pressure. The air flows outwards, increasing the pressure of the surrounding air. See Figure 15.

Depending on how much air flow is generated, where the air flow comes from/goes to, and how large a region is affected, this phenomenon can lead to many different meteorological phenomena. Let us briefly review some of the main types of weather events.

3.4.1 Cyclonic and anti-cyclonic behaviour

One of the main factors studied by meteorologists in weather prediction is the interaction between high pressure systems ("highs" or anti-cyclones) and low pressure systems ("lows" or cyclones), where the pressure referred to is typically the sea level pressure (often given in millibar, *mb*, where 1 mb=100 Pa). Low pressure systems are generally associated with high wind speeds, warm air and high precipitation, while high pressure systems tend to lead to calm, settled conditions with cooler temperatures. In the weather chart in Figure 16, the highs and lows are labelled "H" and "L" respectively.

If the phase change boundary drops in altitude (Figure 14), and the ensuing air flow comes from the ground upwards, this would create an area of low pressure at ground level. If this upward moving air is of high humidity, then the reduction of the air temperature with height (Section 3.1) would cause precipitation. Converting water vapour to rain would also cause a reduction in molar density, reducing the ground pressure further.

That is, a sudden drop in the phase change boundary can lead to cyclonic conditions. Similarly, if the phase change boundary rapidly increases in altitude (Figure 15), this can lead to anti-cyclonic conditions.

Higher or lower pressures at sea level could in turn alter the pressures at the phase change boundary, thereby leading to dynamic feedbacks between the upper and lower tropospheric conditions.

It is not yet clear just how large a role multimerization plays in the cyclonic and anti-cyclonic weather systems. However, if a strong correlation between the changing location of the phase change boundary and sea level pressures can be identified, then this could lead to better weather prediction.

3.4.2 Tropical cyclones and other synoptic scale cyclones

When a low pressure cyclonic system forms over warm tropical oceans, this sometimes leads to the formation of a *tropical cyclone*. Depending on where the tropical cyclone forms it is called either a *"hurricane"*

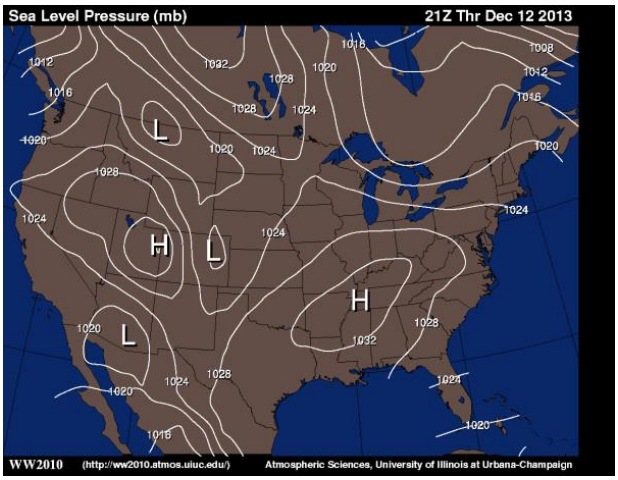

Figure 16: *Weather chart illustrating sea level pressure for the U.S. on 12th December 2013 (21Z). Image from the University of Illinois WW2010 Project.*

(North Atlantic or eastern North Pacific), *"typhoon"* (western North Pacific), or *"cyclone"* (all other ocean basins). Lower intensity versions of a tropical cyclone are known as *"tropical storm"* or *"tropical depression"*, depending on their strength. If one of these storms moves to a higher latitude, or is formed at a higher latitude, it is an *"extra-tropical cyclone"* or a *"depression"*.

Tropical cyclones are large scale ("synoptic") weather systems that can be several hundred kilometres in diameter, and reach up to just below the tropopause, i.e., the phase change boundary. Figure 17 shows a satellite photo of 2003's "Hurricane Isabel". Due to the very high wind speeds, storm surges, heavy rainfall and thunderstorms associated with tropical cyclones, they can be very destructive, particularly if they make landfall.

Until now it has been generally assumed that the main energy source ("fuel") for tropical cyclogenesis comes from the evaporation of warm ocean waters, e.g., Goldenberg et al., 2001[53]; Emanuel, 2005[54]; Webster et al., 2005[55]; Knutson et al., 2010[56]. When the warm water vapour rises up in the atmosphere, it cools down, and condenses out as precipitation, reducing the pressure. This reduction in pressure leads to further water evaporation, and acts as a positive feedback, increasing the intensity of the cyclone. In effect, tropical cyclones are assumed to form "from the bottom up", i.e., the cyclonic conditions start at the ocean surface.

We agree that the evaporation of warm ocean waters can help convert a regular low pressure cyclonic system into a high intensity tropical cyclone. However, we suggest that the initial cyclonic conditions arise out from a sudden fall in the phase change boundary, as described in Section 3.4.1.

Figure 17: *Satellite photo of the tropical cyclone "Hurricane Isabel" about 400 miles north of Puerto Rico on 14th September 2003 (14:45 UTC). Image by Jacques Descloitres, MODIS Rapid Response Team, NASA/GSFC. It is in the public domain, and was downloaded from Wikimedia Commons.*

As the world's population has increased and more people are living in at-risk coastal areas, there has been a substantial increase in the *damage caused* by tropical cyclones in recent decades, e.g., Pielke et al., 2008[57]. This trend is likely to continue in the future, whether or not there are any changes in tropical cyclonic activity - see Knutson et al., 2010 for a discussion of tropical cyclone trends[56]. Hence, improvements in the preparation for and response to tropical cyclones would be desirable. In this context, further research into the relationship between changes in the phase change boundary and tropical cyclogenesis might lead to improvements in tropical

cyclone monitoring and prediction.

Tropical cyclone activity in one part of the world might have implications for weather patterns in other parts of the world. For instance, Landsea & Gray, 1992 suggested that intense tropical cyclone activity in the North Atlantic is associated with heavy rainfall in the Sahel[58]. If such correlations (either causative or commensal) transpire to be robust, then a better insight into tropical cyclogenesis could also provide insights into other weather patterns, such as the alternation between drought and non-drought periods in the Sahel.

3.4.3 Tornadoes and other micro-scale cyclones

During thunderstorms, low pressure systems can also give rise to smaller scale ("micro-scale") weather systems, such as *"tornadoes"* (e.g., Figure 18) or *"waterspouts"* (e.g., Figure 19). Tornadoes are narrow (e.g., < 100m) rotating columns of air with very high wind speeds that suck air from the ground up to the base of the thunderstorm clouds. Waterspouts are a similar phenomenon which occur over bodies of water.

Figure 18: *One of several tornadoes observed by the VORTEX-99 team on May 3, 1999, in central Oklahoma. Photo was taken by Daphne Zaras. It is in the public domain, and was downloaded from Wikimedia Commons.*

Tornadoes are often associated with *"supercells"*, which are a large thunderstorm system that contain a *"mesocyclone"*, where a mesocyclone is a rotating vortex of air with an upward flow. The dome (*"overshooting top"*) of a supercell reaches to the top of the troposphere, i.e., to the phase change boundary. For this reason, we suggest that the pressure change

Figure 19: *A waterspout off the Florida Keys, Florida (USA) on 10th September 1969 photographed from an aircraft by Dr. Joseph Golden (NOAA). It is in the public domain, and was downloaded from the NOAA Photo Library. Credit: National Oceanic and Atmospheric Administration/Department of Commerce.*

caused by a sudden drop in the phase change boundary might be responsible for generating the upward air flow of the mesocyclone needed to form a supercell.

As with tropical cyclones, the average annual damage caused by tornadoes in general increases as the world's population and the value of property and infrastructure exposed to tornado events increases, e.g., see Simmons et al., 2013[59]. So, if the phase change boundary plays a role in the formation of tornadoes and other similar micro-scale cyclones, then research into this relationship could be of considerable societal benefit.

3.4.4 Jet streams

Research in the early-to-mid-20th century revealed the recurring phenomenon of regions of very high horizontal wind speeds (30-100m s^{-1} or faster) in the upper troposphere, near the tropopause[60]. These high wind speed bands of the atmosphere, known as the *"jet streams"*, generally travel thousands of kilometres from west to east and are a few hundred kilometres in width at their maximum, but have a meandering and discontinuous shape, as illustrated schematically in Figure 20. The jet streams tend to be most pronounced during the winter. Recently, there has been an increasing interest in the jet streams, since their location appears to significantly influence tropospheric weather, through *"atmospheric blocking"*[61–

64].

Figure 20: *Schematic depiction of the jet streams. The image was generated by Lyndon State College Meteorology and is in the public domain. It was downloaded from the Wikimedia Commons website.*

There are two main tropospheric jet streams in each hemisphere:

1. The polar jets which occur in the regions between the mid-latitudes and the poles.

2. The subtropical jets which occur in the regions between the mid-latitudes and the tropics.

These regions correspond to quite strong temperature fronts, where cold air masses meet warm air masses. According to the conventional explanation, since hot air is slightly less dense than cold air (all else being equal), the horizontal temperature differences between adjacent air masses at these fronts creates a horizontal pressure gradient, which causes high wind speeds, i.e., the jet streams. The larger the temperature differences, the stronger the wind speeds. The direction of these winds is from west to east because of the Coriolis force.

In light of our discussion of the phase transition, there is an alternative explanation, however. From analysing the relationship between horizontal wind speed and the phase transition, we have found that the highest wind speeds of the jet stream usually occur close to the location of the phase transition. This can be partially seen from Figure 21 (next page), which compares the variation of wind speeds and molar density to pressure for the same seven Valentia Observatory (Ireland) radiosondes considered in Figure 1.

The Valentia Observatory station is located below a region in which the jet stream frequently meanders. In five of the seven plots, high wind speeds occur on either side of the phase transition, and the peak occurs at or near the phase transition. In the remaining two plots, wind speeds are relatively low over the entire atmospheric profile.

Analysis of the video of all radiosondes for the same station in 2012 (provided at http://www.youtube.com/watch?v=UNvjqyvM0gM as Supplementary Information) shows this is a recurring motif. When high wind speeds occur for the Valentia Observatory radiosondes, their maximum usually occurs near the phase transition[9]. This suggests to us that the two phenomena are related.

We suggest that the jet streams occur when the air flow generated by a rise or fall in the phase change boundary occurs horizontally (instead of vertically as in the previous examples). That is, the air flows to/from the sides, just below the phase change boundary. This flow would be acted on by the Coriolis forces in the same manner as in the conventional explanation, and hence could lead to the prevailing westerly winds associated with the jet streams.

We saw from Figure 4 that the location of the phase transition for a given latitude is seasonally dependent. We would therefore expect that the jet streams will be strongest during periods when the location of the phase transition rapidly changes, and be weakest during periods when the location of the phase transition is fairly constant.

It is worth noting that the paths of tropical and extra-tropical cyclones are often "blocked" by the jet streams. We suggest that the jet streams do not actually block cyclone paths. Rather, the jet streams occur in regions where the air flow associated with changes in the phase change boundary altitude is horizontal, whereas the air flow is vertical for cyclones (Section 3.4.2).

3.4.5 Polar vortices

Finally, it may be worth briefly discussing the polar vortex phenomenon. A polar vortex is a large-scale cyclone which often occurs near the poles, and is particularly strong during the polar winter.

Unlike the tropical and extra-tropical cyclones which occur at ground level, the polar vortices are located in the mid-to-upper troposphere and the stratosphere. However, like the other cyclones, they do not occur near the jet streams.

[9] Although higher wind speeds occasionally occur in the stratosphere.

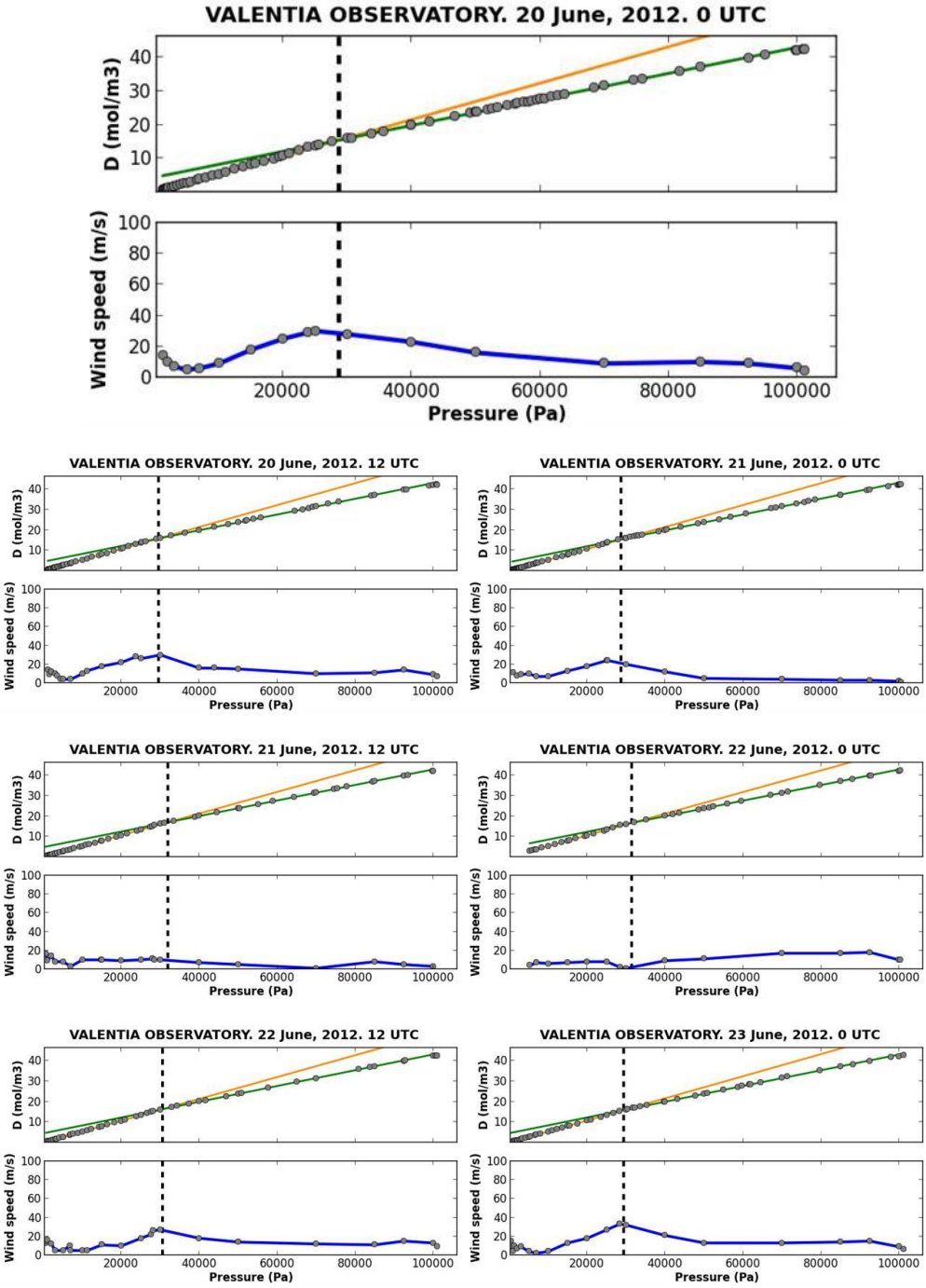

Figure 21: *Comparison between horizontal wind speeds and the molar density plots from the same series of radiosonde balloons shown in Figure 1. The green and yellow lines in the D versus P panels correspond to the linear slopes of the upper and lower regions. The dashed lines indicate the point of intersection of the two regions, and therefore represents the phase transition for each radiosonde. Circles correspond to the weather balloon measurements.*

In Paper I, we noticed that during the Arctic winter, the "heavy phase" occurs in two regions[1]. As well as occurring above the onset of the tropopause, the heavy phase also occurs in the lower troposphere.

If the heavy phase does indeed involve the formation of multimers, as we argue in this paper, then this suggests that multimers also form in the lower troposphere during polar winters. This could explain why the polar vortices occur at higher altitudes than conventional cyclones.

If so, then studying both phase change boundaries might be necessary to properly understand (and ultimately predict) the behaviour of the polar vortices.

4 Final Remarks

In a companion paper (Paper I[1]), we identified a pronounced phase transition associated with the change from the troposphere to the tropopause/stratosphere regions. In this paper, we proposed that this phase change involves the multimerization of oxygen and nitrogen molecules in the tropopause/stratosphere, i.e., the formation of $(O_2)_n$, $(N_2)_n$ or $(O_2)_{n-x}(N_2)_x$, where $n > 1$ and $x < n$.

In the equatorial and sub-tropical regions, we found that the pressure and temperature conditions corresponding to the phase transition varied very linearly with season. For this reason, we were able to estimate the heats of formation associated with the phase transition in these regions. From these estimates we calculated values of n in the range 4.2-4.4 for the multimers, for these regions. This suggests that the multimers include tetramers ($n = 4$) at low latitudes.

In the Antarctic regions, the relationship between the pressure and temperature of the phase transition was also strongly linear. Hence, we also estimated n for these regions. However, while our estimates yielded $n = 3.99$ for the $60 - 75°S$ zone (again suggesting tetramers), for the more southerly $75 - 90°S$ zone, n appeared to be in the range 5.71-5.98. This might indicate the presence of hexamers ($n = 6$), but it could also indicate a mixture of different sized multimers.

For the other zones, the relationships between the pressures and temperatures of the phase transitions were more complex, and so attempting to estimate n from the phase transition conditions appeared too subjective and arbitrary for the available data. Nonetheless, our preliminary estimates suggest that n could be as high as 10-20 for some parts of the year for the extra-tropical Northern Hemisphere, at least.

The existence of a substantial amount of oxygen and/or nitrogen multimers in the tropopause/stratosphere regions has a number of important implications for our current understanding of atmospheric chemistry and physics. In Section 3, we discussed some of these implications.

In Section 3.1, we showed how multimer formation is able to explain why the altitudinal temperature lapse rate is not negative at the tropopause, and is positive in the stratosphere. We believe this explanation is more likely than the conventional explanation that it is due to solar heating of the ozone layer.

In Section 3.2, we explained how the formation of oxygen multimers should lead to microwave and infra-red emissions from the tropopause/stratosphere regions. We also presented an alternative framework for explaining the observed outgoing longwave terrestrial radiation spectra, which is compatible with our finding in Paper I[1] that the troposphere/tropopause/stratosphere regions are in thermodynamic equilibrium, and not just local thermodynamic equilibrium (as is assumed by the conventional framework[3]).

In Section 3.3, we proposed an alternative mechanism for the formation of stratospheric ozone to the conventional Chapman mechanism. We suggest that most of the ozone in the ozone layer is formed by the photolysis of oxygen multimers. This appears to be confirmed by the fact that the seasonal variability in ozone concentrations at different latitudinal zones is highly correlated to the seasonal and latitudinal variability in the phase transition conditions.

The Chapman mechanism is a fairly slow mechanism for the formation of ozone in the ozone layer. In contrast, the photolysis of oxygen multimers should be a rapid mechanism for ozone formation.

This lessens the concern that the build-up of chlorofluorocarbon molecules in the upper atmosphere might have been causing ozone depletion. Although chlorofluorocarbon concentrations do seem to have risen over the 20th century, and chlorine radicals formed from the photolysis of chlorofluorocarbons in the upper atmosphere can destroy ozone molecules, the rate of ozone formation from oxygen multimer photolysis seems to be greater. Instead, much of the observed decrease in average ozone concentrations during the late 20th century is probably due to changes in the phase transition conditions.

The photolysis of nitrogen-oxygen mixed multimers might also lead to the formation of some of the "NO_y" nitrogen oxide compounds commonly associ-

ated with the ozone layer.

Finally, in Section 3.4, we suggest that when the altitude of the phase transition boundary rapidly rises or falls, this can lead to a number of different meteorological phenomena, e.g., cyclonic/anti-cyclonic conditions, tropical cyclones, polar vortices and the jet streams. Hence, studying the phase transition boundary changes should offer useful insights for meteorologists, and perhaps lead to better weather prediction.

Acknowledgements

No funding was received for this research.

We would like to thank Dr. Imelda Connolly for assistance in the construction of several of the figures in this article. We would also like to thank Don Zieman, Dr. Lorraine Nolan and Dr. Anton O'Connor for some useful feedback and discussions.

References

[1] M. Connolly and R. Connolly. "The physics of the Earth's atmosphere I. Phase change associated with tropopause". 19 (Atm. Sci.). Ver. 0.1 (non peer reviewed draft). 2014. URL: http://oprj.net/articles/atmospheric-science/19.

[2] M. Connolly and R. Connolly. "The physics of the Earth's atmosphere III. Pervective power". 25 (Atm. Sci.). Ver. 0.1 (non peer reviewed draft). 2014. URL: http://oprj.net/articles/atmospheric-science/25.

[3] R. T. Pierrehumbert. "Infrared radiation and planetary temperature". *Phys. Today* 64 (2011), pp. 33–38. DOI: 10.1063/1.3541943.

[4] R. W. Spencer and J. R. Christy. "Precise monitoring of global temperature trends from satellites". *Science* 247 (1990), pp. 1558–1562. DOI: 10.1126/science.247.4950.1558.

[5] J. E. Harries et al. "Increases in greenhouse forcing inferred from the outgoing longwave radiation spectra of the Earth in 1970 and 1997". *Nature* 410 (2001), pp. 355–357. DOI: 10.1038/35066553.

[6] S. Chapman. "A theory of upper-atmospheric ozone". *Mem. Roy. Meteor. Soc.* 3 (1930), pp. 103–125. URL: http://www.rmets.org/sites/default/files/chapman-memoirs.pdf.

[7] I. Durre, R. S. Vose, and D. B. Wuertz. "Overview of the Integrated Global Radiosonde Archive". *J. Clim* 19 (2006), pp. 53–68. DOI: 10.1175/JCLI3594.1.

[8] J. B. West. "Prediction of barometric pressures at high altitudes with the use of model atmospheres". *J. Appl. Physiol.* 81 (1996), pp. 1850–1854. URL: http://jap.physiology.org/content/81/4/1850.abstract.

[9] A. Berger, M.-F. Loutre, and C. Tricot. "Insolation and Earth's orbital periods". *J. Geophys. Res. D* 98 (1993), pp. 10341–10362. DOI: 10.1029/93JD00222.

[10] A. Berger. "Milankovitch theory and climate". *Rev. Geophys.* 26 (1988), pp. 624–657. DOI: 10.1029/RG026i004p00624.

[11] N.O.A.A., N.A.S.A., and U.S.A.F. *U.S. Standard Atmosphere 1976*. U.S. Government Printing Office. Washington, D.C., U.S., 1976, 227 pp. URL: http://ntrs.nasa.gov/archive/nasa/casi.ntrs.nasa.gov/19770009539_1977009539.pdf.

[12] C. A. Long and G. E. Ewing. "The infrared spectrum of bound state oxygen dimers in the gas phase". *Chem. Phys. Lett.* 9 (1971), pp. 225–229. DOI: 10.1016/0009-2614(71)85036-4.

[13] A. Campargue et al. "Rotationally resolved absorption spectrum of the O_2 dimer in the visible range". *Chem. Phys. Lett.* 288 (1998), pp. 734–742. DOI: 10.1016/S0009-2614(98)00294-2.

[14] V. Aquilanti et al. "Molecular beam scattering of aligned oxygen molecules. The nature of the bond in the $O_2 - O_2$ dimer". *J. Am. Chem. Soc.* 121 (1999), pp. 10794–10802. DOI: 10.1021/ja9917215.

[15] V. Aquilanti et al. "Dimers of the major components of the atmosphere: Realistic potential energy surfaces and quantum mechanical prediction of spectral features". *Phys. Chem. Chem. Phys.* 3 (2001), pp. 3891–3894. DOI: 10.1039/B106672M.

[16] Z. Slanina et al. "Computing molecular complexes in Earth's and other atmospheres". *Phys. Chem. Earth (C)* 26 (2001), pp. 505–511. DOI: 10.1016/S1464-1917(01)00038-1.

[17] K. Pfeilsticker et al. "First atmospheric profile measurements of UV/visible O_4 absorption band intensities: Implications for the spectroscopy and the formation enthalpy of the $O_2 - O_2$ dimer". *Geophys. Res. Lett.* 28 (2001), pp. 4595–4598. DOI: 10.1029/2001GL013734.

[18] T. Wagner et al. "UV-visible observations of atmospheric O_4 absorptions using direct moonlight and zenith-scattered sunlight for clear-sky and cloudy sky conditions". *J. Geophys. Res. D* 107 (2002), pp. 44244595–4598. DOI: 10.1029/2001JD001026.

[19] O. B. Gadzhiev et al. "Structure, energy and vibrational frequencies of oxygen allotropes O_n ($n \leq 6$) in the covalently bound and van der Waals forms: ab initio study at the CCSD(T) level". *J. Chem. Theory Comput.* 9 (2013), pp. 247–262. DOI: 10.1021/ct3006584.

[20] Yu. A. Freiman and H. J. Jodi. "Solid oxygen". *Phys. Rep.* 401 (2004), pp. 1–228. DOI: 10.1016/j.physrep.2004.06.002.

[21] P. G. Niklowitz et al. "Physisorption of molecular oxygen on C_60 thin films". *J. Chem. Phys.* 120 (2004), p. 10225. DOI: 10.1063/1.1737734.

[22] M. N. Berberan-Santos, E. N. Bodunov, and L. Pogliani. "On the barometric formula". *Am. J. Phys.* 65 (1996), pp. 404–412. DOI: 10.1119/1.18555.

[23] B. A. Tinsley, G. B. Burns, and L. Zhou. "The role of the global electric circuit in solar and internal forcing of clouds and climate". *Adv. Space Res.* 40 (2007), pp. 1126–1139. DOI: 10.1016/j.asr.2007.01.071.

[24] R. G. Barry and R. J. Chorley. *Atmosphere, weather and climate*. 6th. Routledge. London. New York., 1992, 392 pp. ISBN: 0-415-07761-3.

[25] M.-D. Chou. "A solar radiation model for use in climate studies". *J. Atmos. Sci.* 49 (1992), pp. 762–772. DOI: 10.1175/1520-0469(1992)049<0762:ASRMFU>2.0.CO;2.

[26] J. T. Kiehl and K. E. Trenberth. "Earth's annual global mean energy budget". *Bull. Amer. Meteor. Soc.* 78 (1997), pp. 197–208. DOI: 10.1175/1520-0477(1997)078<0197:EAGMEB>2.0.CO;2.

[27] K. E. Trenberth, J. T. Fasullo, and J. Kiehl. "Earth's global energy budget". *Bull. Amer. Meteor. Soc.* 90 (2009), pp. 311–323. DOI: 10.1175/2008BAMS2634.1.

[28] V. Ramanathan et al. "Cloud-radiative forcing and climate: results from the Earth Radiation Budget Experiment". *Science* 243 (1989), pp. 57–63. DOI: 10.1126/science.243.4887.57.

[29] J. Tyndall. "The Bakerian Lecture: On the absorption and radiation of heat by gases and vapours, and on the physical connexion of radiation, absorption, and conduction". *Phil. Trans. Roy. Soc. London* 151 (1861), pp. 1–36. URL: http://www.jstor.org/stable/108724.

[30] H. A. Gebbie et al. "Atmospheric transmission in the 1 to 14μ region". *Proc. R. Soc. Lond. A* 206 (1951), pp. 87–107. DOI: 10.1098/rspa.1951.0058.

[31] P. R. Christensen and J. C. Pearl. "Initial data from the Mars Global Surveyor thermal emission spectrometer experiment: observations of the Earth". *J. Geophys. Res. E* 102 (1997), pp. 10875–10880. DOI: 10.1029/97JE00637.

[32] R. Spang, J.J. Remedios, and M. P. Barkley. "Colour indices for the detection and differentiation of cloud types in infra-red limb emission spectra". *Adv. Space Res.* 33 (2004), pp. 1041–1047. DOI: 10.1016/S0273-1177(03)00585-4.

[33] G. E. Hunt. "Radiative properties of terrestrial clouds at visible and infra-red thermal window wavelengths". *Q. J. R. Meteor. Soc.* 99 (1973), pp. 346–369. DOI: 10.1002/qj.49709942013.

[34] W. J. Wiscombe. "Improved Mie scattering algorithms". *Appl. Opt.* 19 (1980), pp. 1505–1509. DOI: 10.1364/AO.19.001505.

[35] J. H. van Vleck. "The absorption of microwaves by oxygen". *Phys. Rev.* 71 (1947), pp. 413–424. DOI: 10.1103/PhysRev.71.413.

[36] F. S. Rowland. "Stratospheric ozone depletion". *Phil. Trans. R. Soc. B* 361 (2006), pp. 769–790. DOI: 10.1098/rstb.2005.1783.

[37] S. Solomon. "Stratospheric ozone depletion: a review of concepts and history". *Rev. Geophys.* 37 (1999), pp. 275–316. DOI: 10.1029/1999RG900008.

[38] R. L. Miller et al. "The "ozone deficit" problem: $O_2(X, v \geq 26) + O(^3P)$ from 226-nm ozone photodissociation)". *Science* 265 (1994), pp. 1831–1838. DOI: 10.1126/science.265.5180.1831.

[39] A. W. Brewer. "Evidence for a world circulation provided by the measurements of helium and water vapour distribution in the stratosphere". *Quat. J. Roy. Meteor. Soc.* 75 (1949), pp. 351–363. DOI: 10.1002/qj.49707532603.

[40] G. M. B. Dobson. "Origin and distribution of the polyatomic molecules in the atmosphere". *Proc. R. Soc. Lond. A* 236 (1956), pp. 187–193. DOI: 10.1098/rspa.1956.0127.

[41] J. Eluskiewicz and M. Allen. "A global analysis of the ozone deficit in the upper stratosphere and lower mesosphere". *J. Geophys. Res.* 98D (1993), pp. 1069–1082. DOI: 10.1029/92JD01912.

[42] S. F. Singer. "Ozone depletion theory". *Science* 261 (1993), pp. 1101–1102. DOI: 10.1126/science.261.5125.1101.

[43] M. L. Salby, E. A. Titova, and L. Deschamps. "Changes of the Antarctic ozone hole: Controlling mechanisms, seasonal predictability, and evolution". *J. Geophys. Res.* 117 (2012), p. D10111. DOI: 10.1029/2011JD016285.

[44] C. B. Leovy et al. "Transport of ozone in the middle stratosphere: Evidence for planetary wave breaking". *J. Atmos. Sci.* 42 (1985), pp. 230–244. DOI: 10.1175/1520-0469(1985)042<0230:TOOITM>2.0.CO;2.

[45] M. L. Salby and P. F. Callaghan. "Fluctuations of total ozone and their relationship to stratospheric air motions". *J. Geophys. Res.* 98D (1993), pp. 2715–2727. DOI: 10.1029/92JD01814.

[46] M. L. Salby and P. F. Callaghan. "Systematic changes of Northern Hemisphere ozone and their relationship to random interannual changes". *J. Clim.* 17 (2004), pp. 4512–4521. DOI: 10.1175/3206.1.

[47] M. C. Parrondo et al. "Antarctic ozone variability inside the polar vortex estimated from balloon measurements". *Atmos. Chem. Phys.* 14 (2014), pp. 217–229. DOI: 10.5194/acp-14-217-2014.

[48] M. L. Salby. *Fundamentals of atmospheric physics*. 1st. Academic Press. San Diego. London., 1996, 627 pp. ISBN: 978-0126151602.

[49] S. Brönnimann et al. "Total ozone observations prior to the IGY. I: a history". *Q. J. R. Meteorol. Soc.* 129 (2003), pp. 2797–2817. DOI: 10.1256/qj.02.118.

[50] S. Brönnimann, J. Staehelin, and S. F. G. Farmer. "Total ozone observations prior to the IGY. I: data and quality". *Q. J. R. Meteorol. Soc.* 129 (2003), pp. 2819–2843. DOI: 10.1256/qj.02.145.

[51] R. E. M. Griffin. "Detection and measurement of total ozone from stellar spectra: Paper 2. Historic data from 1935-1942". *Atmos. Chem. Phys.* 6 (2006), pp. 2231–2240. DOI: 10.5194/acp-6-2231-2006.

[52] D. W. Fahey et al. "*In situ* observations of NO_y, O_3, and the NO_y/O_3 ratio in the lower stratosphere". *Geophys. Res. Lett.* 23 (1996), pp. 1653–1656. DOI: 10.1029/96GL01476.

[53] S. B. Goldenberg et al. "The recent increase in Atlantic hurricane activity: causes and implications". *Science* 293 (2001), pp. 474–479. DOI: 10.1126/science.1060040.

[54] K. Emanuel. "Increasing destructiveness of tropical cyclones over the past 30 years". *Nature* 436 (2005), pp. 686–688. DOI: 10.1038/nature03906.

[55] P. J. Webster et al. "Changes in tropical cyclone number, duration, and intensity in a warming environment". *Science* 309 (2005), pp. 1844–1846. DOI: 10.1126/science.1116448.

[56] T. R. Knutson et al. "Tropical cyclones and climate change". *Nature Geosci.* 3 (2010), pp. 157–163. DOI: 10.1038/ngeo779.

[57] R. A. Pielke Jr. et al. "Normalized hurricane damage in the United States: 1900-2005". *Nat. Hazards Rev.* 9 (2008), pp. 29–42. DOI: 10.1061/(ASCE)1527-6988(2008)9:(29).

[58] C. W. Landsea and W. M. Gray. "The strong association between western Sahelian monsson rainfall and intense Atlantic hurricanes". *J. Clim.* 5 (1992), pp. 435–453. DOI: 10.1175/1520-0442(1992)005<0435:TSABWS>2.0.CO;2.

[59] K. M. Simmons, D. Sutter, and R. A. Pielke Jr. "Normalized tornado damage in the United States: 1950-2011". *Env. Hazards* 12 (2013), pp. 132–147. DOI: 10.1080/17477891.2012.738642.

[60] J. M. Lewis. "Ooishi's observation: viewed in the context of the jet stream discovery". *Bull. Amer. Meteor. Soc.* 84 (2003), pp. 357–369. DOI: 10.1175/BAMS-84-3-357.

[61] A. Hannachi, T. Woollings, and K. Fraedrich. "The North Atlantic jet stream: a look at preferred positions, paths and transitions". *Quat. J. Roy. Meteor. Soc.* 138 (2012), pp. 862–877. DOI: 10.1002/qj.959.

[62] J. Vial and T. J. Osborn. "Assessment of atmospheric-ocean general circulation model simulations of winter northern hemisphere atmospheric blocking". *Clim. Dyn.* 39 (2012), pp. 95–112. DOI: 10.1007/s00382-011-1177-z.

[63] T. Woollings and M. Blackburn. "The North Atlantic jet stream under climate change and its relation to the NAO and EA patterns". *J. Clim.* 25 (2012), pp. 886–902. DOI: 10.1175/JCLI-D-11-00087.1.

[64] S. Häkkinen, P. B. Rhines, and D. L. Worthen. "Atmospheric blocking and Atlantic multidecadal ocean variability". *Science* 334 (2011), pp. 655–659. DOI: 10.1126/science.1205683.